EMPIRICAL GROUND MOTION PREDICTION EQUATIONS FOR NORTHERN ITALY USING WEAK AND STRONG MOTION AMPLITUDES, FREQUENCY CONTENT AND DURATION PARAMETERS

Massa M.[(1)], Morasca P.[(2)], Moratto L.[(3)], Marzorati S.[(1)], Costa G.[(3)] and Spallarossa D.[(2)]

[(1)] Istituto Nazionale di Geofisica e Vulcanologia, Sezione di Milano-Pavia, via Bassini, 15, 20133 Milano, Italy.

[(2)] Dipartimento per lo Studio del Territorio e delle sue Risorse, Università di Genova, viale Benedetto XV, 5, 16132 Genova, Italy.

[(3)] Dipartimento di Scienze della Terra, Università di Trieste, via E. Weiss, 1, 34127 Trieste, Italy.

Abstract

The aims of this work are to review the Northern-Italy ground motion prediction equations (hereinafter GMPEs) for amplitude parameters and to propose new GMPEs for frequency content and duration parameters. Approximately 10.000 weak and strong waveforms have been collected merging information from different neighbouring regional seismic networks operating in the last 30 years throughout Northern Italy. New ground motion models, calibrated for epicentral distances ≤ 100 km and for both local (Ml) and moment magnitude (Mw), have been developed starting from a high quality dataset (624 waveforms) which consists of 82 selected earthquakes with Ml and Mw up to 6.3 and 6.5 respectively. The vertical component and the maximum of the two horizontal components of motion have been considered, for both acceleration (PGHA and PGVA) and velocity (PGHV and PGVV) data. In order to make comparisons with the most commonly used prediction equations for the Italian territory (Sabetta and Pugliese, 1996 and Ambraseys et al. 2005a,b hereinafter named SP96 and AM05) the coefficients for acceleration response spectra (SHA and SVA) and for pseudo velocity response spectra (PSHV and PSVV) have been calculated for 12 periods ranging between 0.04 s and 2 s and for 14 periods ranging between 0.04 s and 4 s respectively. Finally, empirical relations for Arias and Housner Intensities (IA, IH) and strong motion duration (DV) have also been calibrated. The site classification based on Eurocode (hereinafter EC8) classes has been used (ENV, 1998). The coefficients of the models have been determined using functional forms with an independent magnitude decay rate and applying the random effects model (Abrahamson and Youngs, 1992; Joyner and Boore, 1993) that allow the determination of the inter-event, inter-station and record-to-record components of variance. The goodness of fit between observed and predicted values has been evaluated using the maximum likelihood approach as in Spudich et al. (1999). Comparing the proposed GMPEs both with SP96 and AM05 it is possible to observe a faster decay of predicted ground motion, in particular for distances greater than 25 km and magnitudes higher than 5.0. The result is a fit improvement of about one order of size for magnitudes spanning from 3.5 to 4.5.

Introduction

Ground motion models are an important piece of information for seismic hazard studies in any region. However the reliability of all GMPEs is strongly influenced by the characteristics of the dataset used to calibrate them. The optimal condition to obtain stable regressions would be to have a large amount of data with a wide distribution of magnitudes, distances and source mechanisms (Douglas, 2003). Unfortunately, this is a very rare case; in fact prediction equations are usually limited to the typical magnitude range observed in the study region that, in general, allows to derive empirical relationships only for strong motion data (Ambraseys et al. 2005a,b; Sabetta and Pugliese, 1987,1996; Tento et al. 1992; Campbell, 1985; Douglas, 2003) or weak motion data (Frisenda et al. 2005; Massa et al., 2007).

The datasets used to calibrate many GMPEs are often enough characterized by an irregular and lacking distribution of data, resulting both in unhomogeneous representations of all magnitude-distance ranges and in the presence of outliers. This may lead to obtain some over or under estimations of predicted data, since the final results are governed by the bulk of the distribution (Molas and Yamazaki, 1995; Crouse et al. 1988). Moreover, the spatial distribution of events and stations may introduce an azimuthal effect on the amplitudes of the ground motion (Campbell and Bozorgnia, 1994). For example, Sabetta and Pugliese (1987) observed an azimuthal dependence for some of their results. This is probably due to the limited number of data points since they used 95 records from 17 earthquakes for the whole Italian territory. To reduce this effect it is important to have a good source-to-station azimuthal coverage.

In the last two years three different regional ground motion models have been developed for the study area in order to investigate the detailed attenuation patterns related to the Western Alps and the Northern Apennines (Frisenda et al., 2005), the Central Alps and the Po Plain (Massa et al., 2007) and the Eastern Alps (Bragato and Slejko, 2005). In particular, GMPEs for Western and Central Northern-Italy have been calibrated using datasets with Ml up to 4.9 and 5.2 respectively; these empirical relations, even though obtained from a large number of records, are strongly dependent on weak motions (Ml < 4.0) and they lead, in particular at short distances (less than 30 km), to underestimations for Ml > 4.5. In contrast the model calibrated for Eastern Italy weights the Friuli sequence too heavily and does not ensure a complete coverage with distance for all considered magnitudes because of the small number of available data. As stated by Douglas (2003) few earthquakes may be a limit in constraining the behaviour of the ground motion equations. Moreover these three GMPEs have been derived starting from datasets characterized both by local magnitude and source-stations distances (hypocentral for Frisenda et al., 2005 and Massa et al., 2007 and epicentral for Bragato and Slejko, 2005) calibrated at regional scale.

In the framework of DPC (Italian Civil Defence)-INGV projects 2004-2006 the information coming from the main seismic networks operating both in Northern Italy regions (e.g. RSNI, Regional Seismic network of North-western Italy; RAF, Accelerometric Friuli Venezia Giulia Network; INGV-

CNT, Centralized National Seismic Network; INGV-MI weak and strong motion stations) and in the neighbouring countries (e.g. ARSO, Seismic Network of Slovenia Republic; SDS-net, Swiss digital Seismic Network) in the last 30 years, has been merged with the aim to improve both the completeness of data with respect to distance and magnitude and the azimuthal coverage.

Given the large amount of data available for this study, careful selection ensured that the number of high quality records is large enough to obtain stable results.

Merging data coming from different networks requires both an homogeneous standardization and post-processing of data: all magnitude values and event locations have been carefully re-checked, with particular attention to the common events. In this work we refer our analysis to the epicentral distance and both to M_l and M_w in order to analyze possible different magnitude dependence for the same dataset.

For Europe regions local magnitude is often used by authors to derive ground motion relations probably because in many cases it is the only magnitude type available (Douglas, 2003). Moment magnitude is typically derived for large events that can be waveform modelled. However many authors try to define relationships between magnitude scales (i.e. Giardini et al., 1997, for Europe regions; Gasperini et al., 2004 for Italian regions). Moment magnitude is physically meaningful because it is directly related to earthquake source physics (slip, fault area, rigidity) and does not saturate for large earthquakes (Hanks and Kanamori, 1979).

Another important factor affecting ground motion predictions is the site classification since the site effects are directly dependent on the local site conditions. Although many choices have been made by other authors (Douglas, 2003), we adopted the site classification proposed in the EC8 code (ENV, 1998), that allows us to use the soil coefficients s1 and s2 (see tables 3-12) for the whole of Northern Italy.

Our selected high quality dataset represents the base input to verify and update the GMPEs commonly used for Northern Italy (SP96 and AM05) for PGA, PGV, SA, PSV. Moreover, we try to obtain a better description of the ground shaking, calibrating models also for parameters more related to damage such as Arias Intensity (IA) (Arias, 1970), Housner Intensity (IH) (Housner, 1952) and strong motion duration (DV) (Vanmarcke and Lai, 1980).

Dataset and processing

The available dataset for this study is composed of about 10.000 weak and strong motion data recorded since 1976 by different regional seismic networks operating in Northern Italy (RSNI, Regional Seismic network of North-western Italy; RAF, Accelerometric Friuli Venezia Giulia Network; INGV-CNT, Centralized National Seismic Network; INGV-MI weak and strong motion stations). In tables 1 the main features of the available weak and strong motion stations (i.e. location, sensor, owner, EC8 soil class) are reported. The velocimetric stations, mainly operating in Western and Central-Northern Italy, consist of different kinds of three-component seismometers

(tables 1) coupled with Lennartz Mars-Lite, Mars88-MC or Reftek 130 digital recorders. The strong motion stations (both analogue and digital), mainly operating in NE Italy, and more recently also in Northern Central Italy, are equipped with Kinemetrics Episensors, SMA-1, and FBA23 accelerometers coupled with Kinemetrics K2, SSA-1 or Etna recorders (tables 1).

Given the large amount of data available, a careful selection was possible, leading us to use of only 82 earthquakes (tables 2) with Ml ranging from 3.5 to 6.3 and a maximum epicentral distance of 100 km, to derive empirical ground motion models. The locations of the selected data are shown in Figure 1 (grey circles). In Figure 2 (see inset in the left upper side) the distribution of magnitude with distance of the selected data (624 maximum horizontal and vertical components, of which 216 with Ml>4.5, both for accelerometric and velocimetric data) is shown.

In this work information concerning epicentral distances and local magnitude were derived from INGV bulletin (URL: http://www.ingv.it). For the most energetic events (Ml>5.0) the CPTI04 (Parametric Catalogue of Italian Earthquakes, URL: http://emidius.mi.ingv.it/CPTI/home.html) was also considered.

It is worth noting that the maximum Ml of the dataset is 6.3 (for the 06/05/1976 Friuli earthquake), which is below the saturation level of about 6.5 of the Ml scale (Lay and Wallace, 1995). We chose to consider a minimum threshold of Ml 3.5 because we wanted to obtain reliable models for the range of magnitude characterizing the region under study. Indeed for industrial areas, as pointed out by Campbell (1989), although small events will not produce peak ground acceleration able to seriously damage structures, they can compromise more sensitive components, such as mechanical and electrical equipment of industrial plant.

In order to obtain GMPEs also for *Mw*, the *Ml* values has been converted by using the relation

$$Mw = 0.812(\pm 0.032)Ml + 1.145(\pm 0.154) \quad (\sigma = 0.25) \qquad (1)$$

proposed in Gasperini et al., 2004. The equation (1), valid for Ml ranging between 3.0 and 7.5, has been derived using Italian earthquakes Mw collected from different worldwide catalogues (i.e. Harvard, INGV, ETH etc.) and comparing their values with Ml calculated from observed amplitude. Some tests performed calculating Mw from coda waves (Morasca et al., 2005) on 20 events with 3.5 < Ml < 5.5 included in our dataset, have proved as Gasperini relation tends to overestimate Mw in particular for Ml up to 4.0. This remark represents an important evaluation when Mw is considered to predict weak motions.

The waveforms related to the 82 events used to calibrate GMPEs were a priori base-line corrected and the effect of the instrument response removed; the data acquisition was performed at a minimum sampling rate of 62.5 samples/s for velocimetric stations (so that a minimum antialias cutoff of 25 Hz was guaranteed) and 100 samples/s for strong motion stations. The waveforms are band-pass filtered with a 4^{th} order acasual Butterworth filter between 0.4-25 Hz and 0.2-25 Hz for

Ml ≤ 4.5 and > 4.5 respectively. Tests performed over several recordings showed that the filtering does not affect either PGA or PGV values (Boore and Bommer, 2005) and allows us to calculate reliable response spectral accelerations for the considered periods (range 0.04s-2.0s). In the case of analogue instruments (ENEL,1977) the filtering was carefully checked by the visual inspection of all Fourier amplitude spectra. Finally velocimetric and accelerometric signals were differentiated and integrated respectively in order to ensure a homogeneous dataset both in velocity and acceleration for different magnitudes and distances. The reliability of this process was verified analyzing stations equipped with different sensors (Nanometrics Trillium 40, Lennartz 5s, Kinemetrics Episensor) coupled both with 18 and/or 24 digital recorders (Lennartz Mars88, Reftek 130) and located in different sites (i.e. CTLE, MILA and SALO belong to class C, B and *A* of the EC8 code respectively). The recorded waveforms were then visually checked in order to avoid biasing peaks coming from saturated signals and application of analytical processes on the background noise.

Ground motion parameters

Peak ground acceleration (PGA), peak ground velocity (PGV), and response spectra were calculated using both the vertical component and the larger of the two horizontal components of ground motion (Sabetta and Pugliese, 1996; Ambraseys et al., 2005a,b). For the amplitude parameters the analysis was carried out using a window-length of 30 sec after P arrivals.

In order to obtain the theoretical offset (a coefficients), some authors have considered both the maximum value of the running vectorial composition of the horizontal time series (Bragato and Slejko, 2005) or the geometric mean of the two horizontal components (i.e. the mean of the logarithm, Campbell, 1997). In order to avoid bias due to the choice of the approch to calculate the coefficient *a*, we have performed some tests comparing the values of *a* obtained considering both the larger of the two horizontal components and the geometric mean of the same ones. The results (very similar values of *a*) are able to demonstrate that the use of the larger of the two horizontal components of the ground motion do not lead to errors due to wrong orientation of the sensors installed in the field (Boore et al., 2006).

Acceleration response spectra, for both horizontal and vertical motions (SHA and SVA), were calculated for 12 periods ranging from 0.04s to 2s, while the pseudo velocity response spectra (PSHV and PSVV), were calculated for 14 periods ranging from 0.04s to 4s; in both cases a standard damping of 5% was applied.

The prediction equations were also calibrated for integral parameters that are more related with damage, as recently demonstrated by Masi et al. (2006). The Arias intensity (Arias, 1970) was calculated as the integral of the squared accelerations, considering the total duration of the maximum horizontal time series. The Housner intensity (Housner, 1952) was calculated as the integral of the pseudo spectral velocity response spectrum between periods of 0.1s and 2.5s; also

in this case a standard damping of 5% was applied. The strong motion duration, an important parameter that may contribute to the performance of structural and geotechnical system during an earthquake, may be defined in various ways. In this work we use the definition given by Vanmarcke and Lai (1980) who define it as proportional to ($IA/PGHA^2$) and well correlated to the strong motion phase of the event.

Recording sites

In the framework of task 3.2 of the recent *GNDT* project (ex National Group for Earthquakes Defence) the Italian territory was classified, considering both the EC8 provisions (after the draft of May 2002, ENV, 2002) and the grouping of the geological information of the 1:500.000 Italian Geological Map, in different soil categories (A, B and C classes) (Bordoni et al. 2003). The aim was to introduce the role of the local geology in seismic hazard evaluation. Following this classification, the 77 stations considered in this study were grouped in:

A) rock, Vs (i.e. mean velocity within the first 30 m of depth and relative to the shear waves) > 800 m/s: Marine clay or other rocks (Lower Pleistocene and Pliocene), Volcanic rock and deposits.

B) stiff soil, 360 < Vs < 800 m/s: Colluvial, alluvial, lacustrine, beach, fluvial terraces, glacial deposits and clay (Middle-Upper Pleistocene). Sand and loose conglomerate (Pleistocene and Pliocene). Travertine (Pleistocene and Holocene).

C) soft soil, Vs < 360 m/s: Colluvial, alluvial, lacustrine, beach and fluvial terraces deposits (Holocene).

For the area close to each seismic station the errors associated with the 1:500.000 scale were evaluated by comparing this map with very detailed geological maps (scale 1:10.000 and 1:5.000). From such a comparison no significant differences were observed. Following the aforementioned subdivision, the available dataset includes 49 stations installed on rock, 19 on stiff soil and only 9 on soft soil (see tables 1). Given the very poor number of records available for stations in C class, only one site coefficient (s2), including both B and C classes, was used in the regression analysis. The coefficient related to rock sites (s1) was constrained to zero for all regressions

Method

The general functional form adopted for modelling the ground motion is represented by the expression

$$f(Y)=a+f_1(M)+f_2(R)+f_3(S)+\varepsilon\,, \qquad (2)$$

In this paper in order to calibrate new GMPEs the equation (2) has been developed following both SP96 (equation 3) and AM05 (equation 4), as reported below:

$$log_{10}(Y) = a+(bM)+c\log_{10}(R^2+d^2)^{1/2}+s1S_A+s2S_{(B+C)}+\varepsilon_r+\varepsilon_{(ev/st)} \qquad (3)$$

$$log_{10}(Y) = a+(bM)+\log_{10}(R^2+d^2)^{1/2}(c+(eM))+s1S_A+s2S_{(B+C)}+\varepsilon_r+\varepsilon_{(ev/st)} \qquad (4)$$

where the equation (4) includes coefficients to consider also a magnitude dependent decay rate. In each equation *Y* represents the ground motion parameter to be predicted (PGHA, PGVA, SHA and SVA expressed in g, PGHV, PGVV, PSHV and PSVV in cm/s, IA in cm/s, IH in cm and DV in s). *M* is magnitude (Ml or Mw), *R* (km) is the epicentral distance and S_A and $S_{(B+C)}$ represent dummy variables referred to the site classification whose value is 1 for rock and stiff/soft soil respectively, and zero otherwise. ε_r is an independent random variable that takes on a specific value for each record; ε_{ev} is an independent random variable that takes on a specific value for each earthquake and ε_{st} is an independent random variable that takes on a specific value for each station; a, b, c, d, e, s1 and s2 are parameters to be determined by regression analysis. The coefficient d is a parameter introduced in the models with the aim of incorporating all the factors tending to limit the motion near the source (e.g., finite strength of the rock), a property referred to as saturation with distance (McGuire, 1977; Joyner and Boore, 1981; Bolt and Abrahamson, 1982), while the coefficient *e* of equation (4) refers to the magnitude-dependence decay rate.

Referring to *f1(M)* of equation (2), we also tested a quadratic magnitude term (Boore et al., 1993, Frisenda et al., 2005), but the corresponding coefficient resulted statistically insignificant for all examined ground motion parameters. In the same way, with the aim to investigate the attenuation due to the geometrical spreading (geometrical attenuation) and to the material damping and scattering (anelastic attenuation), the function *f2(R)* has been initially formulated as:

$$f_2(R) = c\text{Log}_{10}(R) + k(R) \qquad (5)$$

in which $c\text{Log}_{10}(R)$ represents the geometrical attenuation and k(*R*) the anelastic attenuation. According to many papers (i.e. Sabetta and Pugliese, 1996; Boore et al., 1993; Ambraseys et al., 2005), the anelastic attenuation coefficient was found statistically insignificant, with values very close to zero, and it was not considered in the final model.

The lack of available information for a relevant number of seismic sources did not allow us to introduce a dependence on JB distance (i.e. the closest distance from recording site to the surface projection of fault rupture, Joyner and Boore, 1981) in the models; likewise the hypocentral distance was not used in order to avoid further errors related to the focal depth uncertainties.

On the basis of the information from both Harvard Centroid-Moment-Tensor (URL http:// http://www.globalcmt.org/) and European and Mediterranean Regional Centroid-Moment-Tensor (URL http:// http://www.ingv.it/seismoglo/RCMT/), it seems that the strongest events of our selected dataset are all generated by inverse faults (in many cases with a slight transcurrent component). In this way no factor for the earthquake mechanism was introduced in the model, consequently it is implicitly valid for a predominant thrust regime.

To estimate the earthquake-to-earthquake, station-to-station and record-to-record components of variance, following Brillinger and Preisler (1984; 1985) and Abrahamson and Youngs (1992) a random effects model was introduced as:

$$log_{10}\, y_{ij} = f(M_i, r_{ij}, \theta) + \eta_i + \varepsilon_{ij}$$

where y_{ij} is the ground motion parameter; $f(M_i, r_{ij}, \theta)$ represents the attenuation equation where M_i is the magnitude of the event i, r_{ij} is the epicentral distance from source i to site j and θ is the vector of model coefficients. η_i represents the inter-event variation and ε_{ij} represents intra-event variation. They are assumed to be independent normally distributed variables with variance σ_{eve}^2 (earthquake-to-earthquake component of variance) and σ_{rec}^2 (record-to-record component of variance), respectively. The total variance σ_{tot} (tables 3-12) is given by:

$$\sigma_{tot} = (\sigma_{eve}^2 + \sigma_{rec}^2)^{1/2}$$

The dependence on recording site can be also considered and the random effect model takes the form:

$$log10\, y_{ij} = f(M_i, r_{ij}, \theta) + \varepsilon'_{ij} + \varphi_j$$

where φ_j represents the inter-station error, assumed to be independent normally distributed with variance σ_{sta}^2 (station-to-station component of variance), and ε'_{ij} is the intra-station variability, with variance σ_{rec}^2, in analogy to the intra-event term. In this case the total variance σ_{tot} (tables 3-12) is given by:

$$\sigma_{tot} = (\sigma_{sta}^2 + \sigma_{rec}^2)^{1/2}$$

Ground motion models for Northern-Italy earthquakes

As a first step we analyzed the ground motion scaling for each region within Northern Italy to verify possible regional scale differences in our data. In many papers it has been demonstrated that the observed differences in regional ground motion scaling are associated with large epistemic uncertainties due to insufficient data to constrain the median prediction, especially for magnitudes and distances of engineering interest (Douglas, 2004; 2007). Suhadolc and Chiaruttini (1987) demonstrated that differences in crustal structure could strongly affect ground motion attenuation, particularly for distances greater than 100 km. Simple tests performed by overlapping recordings coming from different regions of Northern Italy, selected only for rock sites and for various

magnitude and distance ranges, do not show remarkable differences for both the absolute peak values and the motion scaling.

Considering that the study area is characterized by moderate and energetic events with typical compressional focal mechanisms, we think that a single model obtained from high quality data may represent the ground motion scaling for the whole of Northern Italy.

The final results obtained using an independent magnitude functional form (eq. 3) are shown in figures 3-11 and reported in terms of coefficients in tables 3-12.

In order to validate the results, comparisons with both SP96 and AM05 GMPEs were made for each ground motion parameter plotting observed data of relevant earthquakes considered as reference (all informations related to the earthquekes used to validate the empirical curves are reported in the caption of figure 3). The choice of these events was made considering the number of records and the magnitude range coverage. Concerning the amplitude ground motion parameters, in figures 3 and 4 (panels A and B) the PGHA and PGVA of the reference events are shown together with our GMPEs (hereinafter M07). For both horizontal and vertical components, the fit between the model and the observed data is very good for all ranges of magnitude and distance. It is worth noting how both SP96 (panels C and D) and AM05 (panels E and F) models tend to overestimate the observed values for Ml < 5.0. This effect becomes significant (up to one size of order in logarithmic scale) for events ranging from Ml 3.5 to 4.5. Moreover, with respect to our data the SP96 models overestimate the real values for Ml>5.5 and distances greater than 25 km. This phenomenon is less evident in AM05 models because of the introduction of a magnitude-dependent term (i.e. "e*M"* of eq. 4) in the $f_2(R)$ (see eq. 2).

Although our models agree with AM05 well in the first 20 km, a direct comparison could be biased by possible differences between epicentral and fault distances for the events with Ml > 6.0 and for stations close to the fault projection. For smaller earthquakes epicentral and fault distances are comparable because of the small rupture plane of such events (Ambraseys et al., 2005a, Bindi et al., 2006). In figures 5 and 6 the results for PGHV and PGVV are reported. Also in this case both M07 absolute results (panels A and B) and comparisons with SP96 (panels E and F) lead to the conclusions described for PGA. In this case a comparison with AM05 is not possible, so we propose to compare the model of eq. (3) (panels A and B) with the same one which takes into account a magnitude dependent decay rate (eq. 4) (panels C and D): for the horizontal components eq. (4) slightly underestimates the observed data for all magnitudes, with respect to eq. (3). For vertical data the results are very similar for both models. It is worth noting that, compared to AM05 (a,b), we obtain very low values for the coefficient e of eq. (4): between 0.030 (using Ml) and 0.050 (using Mw) for PGHA and between 0.016 (using Ml) and 0.078 (using Mw) for PGVA; while AM05(a,b) values (using Mw) are 0.314 and 0.206 for PGHA and PGVA respectively. All analyzed ground motion parameters do not show such an evident magnitude dependent decay rate to make indispensable the introduction of magnitude in the attenuation term of the model.

For all parameters taken into account in the new GMPEs it is worth noting how attenuation coefficients c very differ from the unit (see tables 3 to 12), reflecting a remarkable scaling of ground motion with distance. Both the data and the regression approach used in such kind of paper (i.e. Sabetta and Pugliese, 1987; 1996; Boore et al., 1993; Ambraseys et al., 2005a,b; Bragato and Slejko 2005; Massa et al., 2007) are not adequate to simultaneously determine negative geometric and anelastic decay coefficients.

The coefficients *c* and *k* (see eq. 5) enter in the model as parameters of log(*R*) and (*R*); then the correlation between *R* and its logarithm implies a linear relationship between c and k. At the end of the regression processes, if we do not apply any constrain for the geometrical spreading (i.e. c = -1), the values of k result statistically insignificant and c accounts for both the effects of geometrical spreading and anelastic attenuation. In this case c coefficient has not to be considered strictly as a represenrtation of geometrical spreading, because it takes into account also for the contribution of anelastic attenuation. The coefficients in GMPEs, due to the false simplification implicitly present in the model used to perform them, have to be interpreted only with a statistical approach (Hutton and Boore, 1987). Moreover observing the tables related to the spectral parametres (tables 4 to 7 and 9 to 12) it is possible to observe in some cases that c coefficients decrease with increasing frequency. Although in the last years (i.e. Zhu et al., 1991; Castro et al., 1999; 2007; Bindi et al., 2004) a frequency dependence of geometrical spreading has been demonstrated, the change of c could be interpreted as a not negligeble contribution of anelstic attenuation. This thesis is strengthen both to the low values and to the strong frequancy-dependence of the quality factor calculated for many regions of Italy (i.e. Castro et al., 1996; 2002; 2007; Augliera et al., 2004; Bindi et al., 2004).

The values of the coefficient *b* in the magnitude term are higher than those obtained by SP96 and AM05 and in most of the worldwide GMPEs (Atkinson and Boore, 1997) derived for magnitudes higher than 5.5, for which b is generally lower than 0.5. On the contrary, the b values obtained in this work (always higher than 0.65) are comparable to those obtained in other studies where the dataset includes both weak and strong motion recordings (Bindi et al., 2006). We have, however, to take into account that the parameters could be trading off against each other in the used one-step-regression.

Figures 3 to 6 also show the values of event-to-event and station-to-station residuals, related to each event and station used in the regression analysis: the low values of both σ_{eve} and σ_{sta}, never larger than 0.13, (see tables 3-12) point out how well the calibrated models describe the source features of the events. For some parameters, we observed larger values of σ_{sta} probably because for some stations the soil classification does not reflect the real behaviour of the site. In fact, Massa et al. (2007) observed that the EC8 classification could lead to biasing estimations, especially for stations installed in very deep basins (e.g. the Po Plain, with thickness of sediments of about 1 km). In this paper, in order to ensure homogeneous results we chose to consider the EC8 site

classification as official reference; in our case only two stations (6 records for CTLE and 2 for CORT, either included in EC8 C class, table 1) of those installed in the Po Plain (MILA, B class, BUIA, C class, CODR, B class and CONE, B class), show a disagreement between the results coming from spectral analysis (HVSR computed on both noise and earthquakes do not show particular amplification effects, Massa et al., 2007) and EC8 classification. Regarding another particular case, we have to underline as Barnaba et al. (2007) have shown as the records of TOLM station (EC8 A class, table 1) could be affected by possible structure-soil interaction and/or variations due to topographic effects. Some tests performed to verify the dam influence on records of TOLM lead to evidence a weak decrease of the larger peak of horizontal acceleration from 0.350 g to 0.303 g. For this site, in order to take into account also other factors that could affect the records (i.e. topographic effetc), it should be reasonable to add in the predicted values the term $S_2.S_{(b+c)}$, like so for sites which suffer of geological effects. Similar inspections performed for MABI, DIX and BARC (table 1), other stations of our dataset located near a dam, have highligthed the absence of particular variations of values caused by possible soil-structure interaction.

In order to strengthen the meaning of the residuals, box-and-whisker plot are also performed and represented in the aforementioned figures (3 to 6). In this case we have grouped the earthquakes in two classes of local magnitude (minor and major of Ml 4.5) and the stations in two classes of soil conditions (EC8 class A and classes B and C togheter). The boxes show in general good results: in particular for accelerations it is possible to note as for event-residuals the higher values are associated with Ml < 4.6, due to the great amount of data, while for station-residuals the group with higher discards are associated with stiff and soft soil (classes B and C respectively).

In figure 7 the results for IA and IH are shown. Also for Arias Intensity we observed an improvement of the results with respect to SP96, considering all magnitudes and distances > 30 km, and for magnitudes up to about 5.0 and the whole distance range. For Housner Intensity no comparison is possible since there are no relations available at present. However, the ratios calculated between IH and PGHV range between 2.5 and 2.6 are like those obtained by Decanini et al. (2000) in other zones of Italy.

The results for acceleration response spectra (SA) are shown in figures 8 and 9 and for pseudo velocity response spectra (PSV) in figures 10 and 11. All information related to the earthquakes used to validate the spectral models are reported in the caption of figure 8.

SA and PSV models, both for vertical and maximum horizontal components were calibrated considering the same periods of SP96 and AM05: 12 periods ranging from 0.04s to 2s and 14 periods ranging from 0.04s and 4s respectively.

The observed response spectra shown in the figures, are compared to our models and both to SP96 (using Ml) and AM05 (using Mw). For all models the derived synthetic spectra were computed considering near and far field stations both on *rock* and *soil* sites (see figures for details). For SHA and SVA (Fig. 8 and 9), results show a better fit of our curves to the observed

data, with respect to AM05 (for both horizontal and vertical components), in particular for the main events (Mw=6.5) at short distance. Moreover, as shown for amplitude parameters, our models ensure a great improvement of the results for the weak motion predictions, at both short and long distances. For the other events the performance of the two models is comparable. Also in this case it is important to point out that the discrepancies between this study and AM05 results for the Mw 6.5 event recorded at a short distance, might be due to the different distance metric used in this study (epicentral distance) and AM05 (JB distance). For PSV (Fig. 10 and 11) the conclusions are very similar to those for SA. In fact compared to SP96, we observed, for both horizontal and vertical components, a slightly better fit of our model to the main event recorded at short epicentral distances. We also obtained a clear improvement of the predictions for weak motions, in particular for periods from 0.1 to 10 Hz. Also in this case the two models give comparable results for the other events.

All GMPEs were also calibrated using Mw as independent variable (see tables 8-12), and the analysis yielded very similar results (not shown in figures) as those obtained with Ml.

In order to evaluate the residual distribution for eq. (3) and its central tendency the approach of Spudich et al. (1999) was followed. The residuals are defined as the difference between the logarithms of the observed and predicted values, and they are assumed to be normally distributed. Spudich et al. (1999) defined the bias between observed and expected ground-motion parameters as the mean value of the residual distribution; furthermore, they characterized the residuals using basic variables such as the slope of the best fitting line through a set of residuals as a function of magnitude M or distance R (slope of the best fitting functions). Bias and best fitting functions obtained for PGHA, PGVA, PGHV and PGVV are shown in figures 12 versus epicentral distance and local magnitude respectively: in any case the absence of significant trends confirms the goodness of the results. Similar good results (not reported here) were obtained for the other ground motion parameters. Spudich et al. (1999) approach was also used to evaluate the performance of SP96 model with respect to our dataset. As shown in figure 13, for both PGA and PGV the SP96 models over-estimate the predicted values both for magnitudes lower than 5.0 (in particular between 3.5 and 4.5) and for epicentral distances greater than 25 km.

Conclusions

New empirical ground motion prediction equations for Northern Italy were calibrated using an high quality dataset, composed of 82 carefully selected earthquakes characterized by Ml ranging from 3.5 (Mw=4.0) to 6.3 (Mw=6.5) and with epicentral distances up to 100 km. The GMPEs proposed in this work are valid for amplitude (PGA and PGV), frequency content (SA and PSV), integral and duration (IA, IH, DV) parameters of the ground motion. In order to verify the efficiency of the models with respect to the features of seismic sources and to the EC8 site classification, the regression analysis was performed considering the random effects model (Abrahamson and

Youngs, 1992; Joyner and Boore, 1993) that allows for the estimation of the inter-event, inter-station and record-to-record components of variance. The main conclusions of this work can be summarized as follow:

- The ground motion predictive equations obtained in this paper represent a useful tool in the hazard assessment related to the area shown in figure 1 (longitude ranging from about 6°E to 15°E and latitude ranging from about 43°N to 47°N). Their upper application limits are Ml 6.3, Mw 6.5 and epicentral distance 100 km. Given the lacking of data with epicentral distance < 10 km, we recommend to consider, for events with Ml > 5.5, this value of distance as the limit below which the phenomena of the saturation of graund motion near the source starts (i.e. it is clearly evident as, also considering distances < 10 km, predicted values higher than 0.4 g apperas unrealistic for considered Ml).
- The results of this study, reported in figures 3-11 for Ml and for different ground motion parameters, were compared to SP96 and AM05 models: in all cases our relationships (indicated as M07) show a better fit to observed data for magnitude greater than 5.0 and for distances > 25 km. Moreover, a considerable improvement is observed for $M \leq 5.0$ (up to one order of size for M ranging from 3.5 to 4.5). This result is important since the area under study is mainly characterized by weak motion with magnitudes ($M \leq 5.0$) able to produce different kinds of damage (i.e. mechanical and electrical equipment of industrial plants etc.). For example, the recent 25 November 2004 Salò earthquake (Central North Italy), Mw=5.0 (Ml=5.2), produced damage for about 215 million Euro in the epicentral area.
  Very similar results were obtained using Mw: the corresponding ground motion coefficients are indicated in tables 8-12.
- The scaling of data used in this study does not make the introduction of coefficients in the attenuation model necessary to take into account of a magnitude dependent decay rate. Indeed in the case of regressions using eq. (4), we find a very low coefficient e with respect to AM05.
- The c coefficient have not to be interpreted strictly as a geometrical spreading coefficient but as a parameter that includes both the contributions of geometrical and anelastic attenuation. In our case data and processing are not able to reliably separate the contribution of c and k: the not negligeble contribution of anelastic attenuation colud be implicitly demonstrate observing the variations of c in the spectral models at different periods (see tables 4 to 7 and 9 to 12).
- The residual analysis shows that the event-to-event (σ_{eve}) and station-to-station (σ_{sta}) errors are negligible, therefore the magnitude values, the epicentral coordinates and the site classification used for this work are correctly estimated. In a few cases we noted that the EC8 classification is not suitable for stations located on very thick sediments (i.e. Po Plain area). However, the low number of recordings available for the 2 stations (CTLE and CORT) located in the Po Plain does not bias the estimation of the site coefficient s2.

- Since the moment magnitudes used in this study were derived from Ml, using Gasperini et al. (2004) empirical relation, we think that a careful estimation of the seismic moment for the events in our dataset will be necessary to improve the GMPEs using Mw. For future we will calibrate moment magnitudes applying well established coda calibration methodologies (i.e. Mayeda et al. 2003; Morasca et al., 2005).

Aknowledgements

This research has been supported by the Dipartimento della Protezione Civile: project S4, ProCiv-INGV (2004-2006). Particular thanks to Gail Atkinson, Marco Mucciarelli and anonymous reviewer who provided helpful review that improved this article. A thanks to Paolo Augliera (INGV Milano-Pavia), Francesca Bianco (INGV Napoli) and Raul Castro (CICESE) for useful suggestions and to all technicians who manage the weak and strong motion stations used in this study.

References

Abrahamson, N.A. and Youngs, R.R. (1992). A stable algorithm for regression analyses using the random effects model, *Bull Seism. Soc. Am.,*82, 505-510.

Ambraseys, N.N., Douglas, J., Sarma, S.K. and Smit, P.M. (2005a). Equations for estimation of strong ground motions from shallow crustal earthquakes using data from Europe and the Middle East: horizontal peak ground acceleration and spectral acceleration, *Bull. of Earthquake Eng*., 3, 1-53.

Ambraseys, N.N., Douglas, J., Sarma, S.K. and Smit, P.M. (2005b). Equations for estimation of strong ground motions from shallow crustal earthquakes using data from Europe and the Middle East: vertical peak ground acceleration and spectral acceleration, *Bull. of Earthquake Eng*., 3, 55-73.

Arias, A. (1970). A measure of earthquake intensity, in *Seismic Design of Nuclear Power Plants*, R. Hansen (Editor), M.I.T. press, Cambridge.

Atkinson, G.M. and Boore, D.M. (1997). Some Comparisons between Recent Ground-Motion Relations, *Seismological Research Letters* 68(1), pp 24-40.

Augliera, P., D'Alema, E., Marzorati, S., Bindi, D., Maistrello, M. and Gassi, A. (2004). The 2003 data set of seismic waveforms recorded in Lombardia and Veneto regions (Northern Italy): site selection and Ml scale calibration, *Proceedings of XXIX General Assembly of ESC*, Potsdam September 2004, 60.

Barnaba, C., Priolo, E., Vuan, A. and Romanelli, M. (2007). Site effect on the strong motion site at Tolmezzo-Ambiesta dam in Northeastern Italy, *Bull. Seism. Soc Am.*, 97 (1b), 339-346.

Bindi, D., Castro, R.R., Franceschina, G., Luzi, L. and Pacor, F. (2004). The 1997-1998 Umbria-Marche sequence (central Italy): Source, path, and site effects estimated from strong motion data recorded in the epicentral area, *Jour. of Geoph. Res*., 109, B04312, 1-17.

Bindi, D., Luzi, L., Pacor, F., Franceschina, G. and Castro, R.R. (2006). Ground-Motion Prediction from Empirical Attenuation Relationships versus Recorded Data: The Case of the 1997-1998 Umbria-Marches, Central Italy, Strong Motion Data Set, *Bull. Seism. Soc Am.*, 96 (3), 984-1002.

Bolt, B.A. and Abrahamson, N.A. (1982). New attenuation relations for peak and expected accelerations of strong ground motion, *Bull. Seism. Soc. Am.*, 72, 2307-2321.

Bordoni, P., De Rubeis, V., Doumaz, F., Luzi, L., Margheriti, L., Marra, F., Moro, M, Sorrentino, D. and Tosi, P. (2003). Geological class map, in *Terremoti probabili in Italia tra l'anno 2000 e 2030: elementi per la definizione di priorità degli interventi di riduzione del rischio sismico, Annex 1, Task 3.2*, 3-4 pp., GNDT Proj., Rome.

Boore, D.M., Joyner, W.B. and Fumal, T.E. (1993). Estimation of response spectra and peak accelerations from Western North American earthquakes, an interim report, *U.S. Geol.Surv. Open File report*, 93-509.

Boore, D.M. and Bommer, J.J. (2005). Processing of strong-motion accelerograms: needs, options and consequences, *Soil Dynamics and Earthquake Engineering*, 25, 93-115.

Boore D.M., Watson-Lamprey, J. and Abrahamson, A. (2006). Orientation-independent measures of ground motion, *Bull. Seism. Soc. Am.*, 96(4), 1502-1511.

Bragato, P.L. and Slejko, D. (2005). Empirical ground-motion attenuation relations for the Eastern Alps in the magnitude range 2.5-6.3, *Bull. Seism. Soc. Am.*, 95(1), 252-276.

Brillinger, D. R. and H. K. Preisler (1984). An exploration analysis of the Joyner-Boore attenuation data. *Bull. Seism. Soc. Am.,* 74(4), 1441-1450.

Brillinger, D. R. and H. K. Preisler (1985). Further analysis of the Joyner-Boore attenuation data, *Bull. Seism. Soc. Am.,* 75(2), 611-614.

Campbell, K.W. (1985). Strong motion attenuation relations: a ten-year perspective, *Earthquake Spectra*, 1(4), 759–804.

Campbell, K.W. (1989). The difference of peak horizontal acceleration on magnitude, distance, and site effects for small-magnitude earthquakes in California and eastern North America, *Bull. Seism. Soc. Am.*, 79, 1311-1341.

Campbell, K.W. and Bozorgnia, Y. (1994). Empirical Analysis of Strong Ground Motion from the 1992 Landers, California, Earthquake, *Bull. Seism. Soc. Am.*, 84 (3), 573-588.

Campbell, K.W. (1997). Empirical near-source attenuation relationships for horizontal and vertical components of peak ground acceleration, peak ground velocity and pseudo-absolute acceleration response spectra, *Seism. Res. Lett.*, 68(1), 154-180.
Castro, R.R., Pacor, F., Sala, A. and Petrungaro, C. (1996). S wave attenuation and site effects in the region of Friuli, Italy, *Jour. of Geoph. Res.*, 101, B10, 22355-22369.

Castro, R.R., Monachesi, G., Mucciarelli, M., Trojani, L. and Pacor, F. (1999). P- and S-wave attenuation in the region of Marche, Italy, *Tectonophysics*, 302, 123-132.

Castro, R.R., Monachesi, G., Trojani, M., Mucciarelli, M. and Frapiccini, M. (2002). An attenuation study using earthquakes from the 1997 Umbria-Marche sequence, *Jour. of Seism.*, 6, 43-59.

Castro R.R., Massa M., Augliera P. and Pacor F. (2007). Body wave attenuation in the region of Garda, Italy, *PAGEOPH.,* submetted.

Crouse, C.B., Vyas, Y.K. and Schell, B.A. (1988). Ground motion from subduction-zone earthquakes, *Bull. Seism. Soc Am.*, 78 (1), 1-25

Decanini, L., Mollaioli, F., Panza, G.F., Romanelli, F. and Vaccari, F. (2000). Pericolosità sismica della Sicilia Sud Orientale. Terremoti di scenario per Augusta, Siracusa e Noto, in *Decanini, L., and Panza, G.F., "Scenari di pericolosità sismica ad Augusta, Siracusa e Noto"*, CNR-Gruppo Nazionale per la Difesa dei Terremoti - Roma, p. 129.

Douglas, J. (2003). Earthquake ground motion estimation using strong motion records: a review of equations for the estimation of peak ground acceleration and response spectral ordinates, *Earth-Science Reviews,* 61, p. 43-104

Douglas, J. (2004). An investigation of analysis of variance as a tool for exploring regional differences in strong ground motions, *Jour. of Seism.,* 8, 485-496.

Douglas, J. (2007). On the regional dependence of earthquake response spectra, special issue: response spectra, *Jour. of Earthquake technology*, 44 (1), N 477.

ENEL (1977). Strong motion earthquake accelerograms digitized and plotted data - Uncorrected accelerograms - Accelerograms for the Friuli, Italy earthquake of May 6, 1976 and aftershocks. Commissione CNEN-ENEL per lo studio dei problemi sismici connessi con la realizzazione di impianti nucleari. Rome, Italy, November 1977.

ENV 1998, EUROCOD 8 (2002). Design provisions for the earthquake resistance of structures. Seismic action and general requirements of structures, *CEN/TC 250*, Draft, May 2002.

Frisenda, M., Massa, M., Spallarossa, D., Ferretti, G. and Eva, C. (2005). Attenuation relationship for low magnitude earthquakes using standard seismometric records, *Journal of Earth. Eng.*, 9(1), 23-40.

Gasperini, P. and Gruppo di lavoro per redazione della mappa di pericolosità sismica prevista dall'ordinanza PCM 3274 del 20 Marzo 2003 (2004). Catalogo dei terremoti CPTI2 - App. 1 al rapporto conclusivo, *open file report.*, 1-29.

Giardini, D., Di Donato M. and Boschi E. (1997). Calibration of magnitude scales for earthquakes of the Mediterranean, *Jour. of . Seism.*, 1, 161-180.

Hanks, T.C. and Kanamori, H. (1979). A moment magnitude scale, *J. Geophys. Res.,* 84 ,2348-2350.

Housner, G.W. (1952). Spectrum intensities of strong-motion earthquakes, in: *Proc. Symp. on Earthquake and Blast Effects Structures*, C. M. Feigen (editors), Univ. California, Los Angeles, 21-36.

Hutton, L.K. and Boore D.M. (1987). The Ml scale in Southern California, *Bull. Seism. Soc. Am.*, 77(6), 2074-2094.

Joyner, W.B. and Boore, D.M. (1981). Peak horizontal acceleration and velocity from strong motion records including records from the 1979 Imperial Valley, California, *Bull. Seism. Soc. Am.*, 71, 2011-2038.

Joyner, W.B. and Boore, D.M. (1993). Methods for regression analysis of strong-motion data, *Bull. Seism. Soc. Am.*, 83(2), 469-487.

Lay, T. and Wallace, T.C. (1995). Modern Global Seismology, *Academic Press*, 521.

Masi, A., Vona, M. and Mucciarelli, M. (2006). Selezione dell'input sismico per la determinazione della vulnerabilità su base meccanica di edifici in c.a., XXV GNGTS conference, book of abstract, 263-267.

Massa, M., Marzorati, S., D'Alema, E., Di Giacomo, D. and Augliera, P. (2007). Site classification assessment for estimating empirical attenuation relationships for Central-Northern Italy earthquakes, *Journal of Earth. Eng.*, in press.

Mayeda, K., Hofstetter, A., O'Boyle, J.L. and Walter W.R. (2003). Stable and transportable regional magnitudes based on coda moment rate spectra, *Bull. Seism. Soc Am*., 93 (1), 224-239.

McGuire, R.K. (1977). Seismic design spectra and mapping procedures relations, *J. Geotech. Eng. Struct. Dyn.*, 5, 211-234.

Molas, G.L. and Yamazaki, F. (1995). Attenuation of earthquake ground motion in Japan including deep focus events, *Bull. Seism. Soc Am*., 85 (5), 1343-1358.

Morasca, P., Mayeda K., Malagnini, L. and W. R Walter (2005). Coda Derived Source Spectra, Moment Magnitudes, and Energy-Moment Scaling in the Western Alps, *Geophys. Journal Int.* 160 (1), 263-275.

Sabetta, F. and Pugliese, A. (1987). Attenuation of peak horizontal acceleration and velocity from Italian strong-motion records, *Bull. Seism. Soc. Am.*, 77, 1491-1513.

Sabetta, F. and Pugliese, A. (1996). Estimation of response spectra and simulation of non-stationary earthquake ground motions, *Bull. Seism. Soc Am* , 86(2), 337-352.

Spudich, P., Joyner, W.B., Lindh, A.G., Boore, D.M., Margaris, B.M. and Fletcher, J.B. (1999). SEA99: a revised ground motion prediction for use in extensional tectonic regimes, *Bull. Seism. Soc. Am.*, 89, 1156-1170.

Suhadolc P. and Chiaruttini, C. (1987). A theoretical study of the dependence of the peak ground acceleration on source and structure parameters, in: Erdik M. and Toksoz M. (eds.), *Strong ground motion seismology*, D. Reidel Publishing Company, 143-183.

Tento, A., Franceschina, L. and Marcellini A. (1992). Expected ground motion evaluation for Italian sites, *Proceedings of 10th World Conference on Earthquake Engineering,* Madrid, Spain, 19-24 July, 1992, A.A. Balkema, Rotterdam, 1, 489-494.

Toro, G.R., Abrahamson, N.A. and Schneider, J.F. (1997). Model of Strong Ground Motions from Earthquakes in Central and Eastern North America: Best Estimates and Uncertainties, *Seismological Research Letters*, 68, No.1, pp. 41-57.

Vanmarcke, E.H. and Lai, S.P. (1980). Strong motion duration and RMS amplitude of earthquake records, *Bull. Seism. Soc. Am.*, 70, 1293-1307.

Zhu, T., Chun, K.Y. and West, G. (1991). Geometrical spreading and Q of Pn waves: An investigative study in eastern Canada, *Bull. Seism. Soc. Am.*, 81, 882-896.

Captions

Fig. 1 - Location of the 82 earthquakes with Ml ≥ 3.5 recorded at epicentral distances ≤ 100km (grey circles with dimensions proportional to the local magnitude) used in the regression analysis. In the figure all events (black crosses) included in the whole of North-Italy dataset and the available seismic stations (white triangles) are also indicated.

Fig. 2 - Distribution of the North-Italy dataset (grey circles) in terms of local magnitude and epicentral distance. The inset in the upper-left side of the diagram indicates the recordings (306 maximum horizontal records and 306 vertical records) selected for the regression analysis (Ml ≥ 3.5 and epicentral distances ≤ 100 km).

Fig. 3 - Top panels: on the left are shown the standard deviations σ_{eve} (black circles) of the inter-event distribution related to the 82 earthquakes considered in the regression analysis; on the right the standard deviations σ_{sta} (black circles) related to the 77 available seismic stations are shown. Box-and-whisker plots grouping the events in different magnitude and site in different EC8 classes are also reported.

In the other panels comparisons between PGHA (peak ground maximum horizontal acceleration) related to the most significant events of the dataset (in terms of number of records) and empirical curves obtained in this study are shown.

Panel A shows the PGHA values of two events of Ml 5.7 (Mw=5.8) (12/04/1998 10:55:32 and 11/09/1976 16:35:00, white circles) versus the M07 empirical curve calculated for Ml=5.7 (solid and dashed black lines represent the mean value and $\pm \sigma_{tot}$) and for two events of Ml 3.5 (Mw=4.0) and 3.8 (Mw=4.2) (20/11/2005 10:48:58 and 20/10/2006 00:11:58, light grey circles) versus the M07 empirical curve calculated for Ml=3.65 (solid and dashed light grey lines represent the mean value and $\pm \sigma_{tot}$).

Panel B shows the PGHA values of two events of Ml 6.1 (Mw=6.1) and 6.3 (Mw=6.5) (15/09/1976 09:21:18 and 06/05/1976 20:00:12, white circles) versus the M07 empirical curve calculated for Ml=6.2 (solid and dashed black lines represent the mean value and $\pm \sigma_{tot}$) and for two events of Ml 5.1 (Mw=5.0) and 5.4 (Mw=5.5) (14/02/2002 03:18:02 and 11/09/1976 16:31:13, grey circles) versus the M07 empirical curve calculated for Ml=5.25 (solid and dashed grey lines represent the mean value and $\pm \sigma_{tot}$).

In panels C and D the comparison between the same real data and the curves calibrated by SP96 are shown, while in panels E and F the comparison with the GMPEs calibrated by AM05 are shown. In the last case the Mw values, if not available on CPTI04 (http://emidius.mi.ingv.it/CPTI/home.html), were derived by considering the relation proposed in Gasperini et al., 2004.

Fig. 4 - The same as in figure 3 but for PGVA (peak ground vertical acceleration).

Fig. 5 - The same as in figure 3 but for PGHV (peak ground maximum horizontal velocity). In panels A and B the M07 empirical curves obtained in this study by using the equation (3) (magnitude independent functional form) are reported, while in panels C and D the results obtained by introducing in the regression analysis a magnitude-dependent functional form (equation 4) are shown. In panels E and F the peak values versus the empirical curves calibrated by SP96 are shown.

Fig. 6 - The same as in figure 5 but for PGVV (peak ground vertical velocity).

Fig. 7 - Comparison between values of IA (Arias Intensity, upper and middle left panels) and IH (Housner intensity, bottom panels), calculated for the events considered in the previous figures (3, 4, 5 and 6), and the curves obtained in this study. For Arias intensity the comparison between observed data and SP96 GMPEs are also shown (upper and middle right panels).

Fig. 8 - Top panels: SHA (spectral horizontal acceleration, black solid lines) for the 06/05/1976 20:00:12 event (Ml=6.3; Mw=6.5) recorded at a “rock” site, with epicentral distance of 23 km (upper left panel), and for the 11/09/1976 16:35:00 event (Ml=5.7; Mw=5.8) recorded at a “soft” site, with epicentral distance of 15 km (upper right panel); in each panel comparison with spectral acceleration estimated in this study (light gray lines with dots) and with those estimated in AM05 (dark grey lines with dots) are shown. In the two middle panels the results for the same two events, but recorded at a “rock” site with epicentral distance of 42 km and 49 km respectively, are reported. In the two bottom panels the results related to the 20/10/2006 00:11:58 weak motion recorded at a “soil” site with epicentral distance of 20 km and at a “rock” site with epicentral distance of 53 km are shown.

Fig. 9 - The same as in figure 8 but for SVA (spectral vertical acceleration).

Fig. 10 - The same as in figure 8 but for PSHV (pseudo-spectral horizontal velocity). In this case the comparison was made by considering the GMPEs calibrated in SP96.

Fig. 11 - The same as in figure 10 but for PSVV (pseudo-spectral vertical velocity).

Fig. 12 - Residuals for PGHA, PGVA, PGHV and PGVV (logarithm for observations minus logarithm of predictions) estimated by the regressions performed considering equations (3) and

calculated versus epicentral distance and local magnitude. In each panel both bias (solid dark grey lines) and the residuals best fit functions are reported.

Fig. 13 - Bias (solid and dashed grey lines for mean values and standard deviations respectively) and fitting functions (solid black lines) calculated considering our data (grey circles) and both PGA and PGV SP96 GMPEs (both for horizontal and vertical components).

Table 1a, 1b - Description of the stations considered in this study.

Table 2a, 2b - Description of the earthquakes considered in this work for the regression analysis. The number of records for each event takes into account horizontal and verical waveforms of both accelerometric and velocimetric signals.

Table 3 - Regression coefficients for PGHA, PGVA, PGHV, PGVV, IA, IH and DV (Vanmarcke and Lai, 1980) calculated for epicentral distances and local magnitude for equation 3.

Table 4 - Regression coefficients for SHA, calculated for epicentral distances and local magnitude for equation 3.

Table 5 - Regression coefficients for SVA, calculated for epicentral distances and local magnitude for equation 3.

Table 6 - Regression coefficients for PSHV, calculated for epicentral distances and local magnitude for equation 3.

Table 7 - Regression coefficients for PSVV, calculated for epicentral distances and local magnitude for equation 3.

Table 8 - Regression coefficients for PGHA, PGVA, PGHV, PGVV, IA, IH and DV calculated for epicentral distances and moment magnitude for equation 3.

Table 9 - Regression coefficients for SHA, calculated for epicentral distances and moment magnitude for equation 3.

Table 10 - Regression coefficients for SVA, calculated for epicentral distances and moment magnitude for equation 3.

Table 11 - Regression coefficients for PSHV, calculated for epicentral distances and moment magnitude for equation 3.

Table 12 - Regression coefficients for PSVV, calculated for epicentral distances and moment magnitude for equation 3.

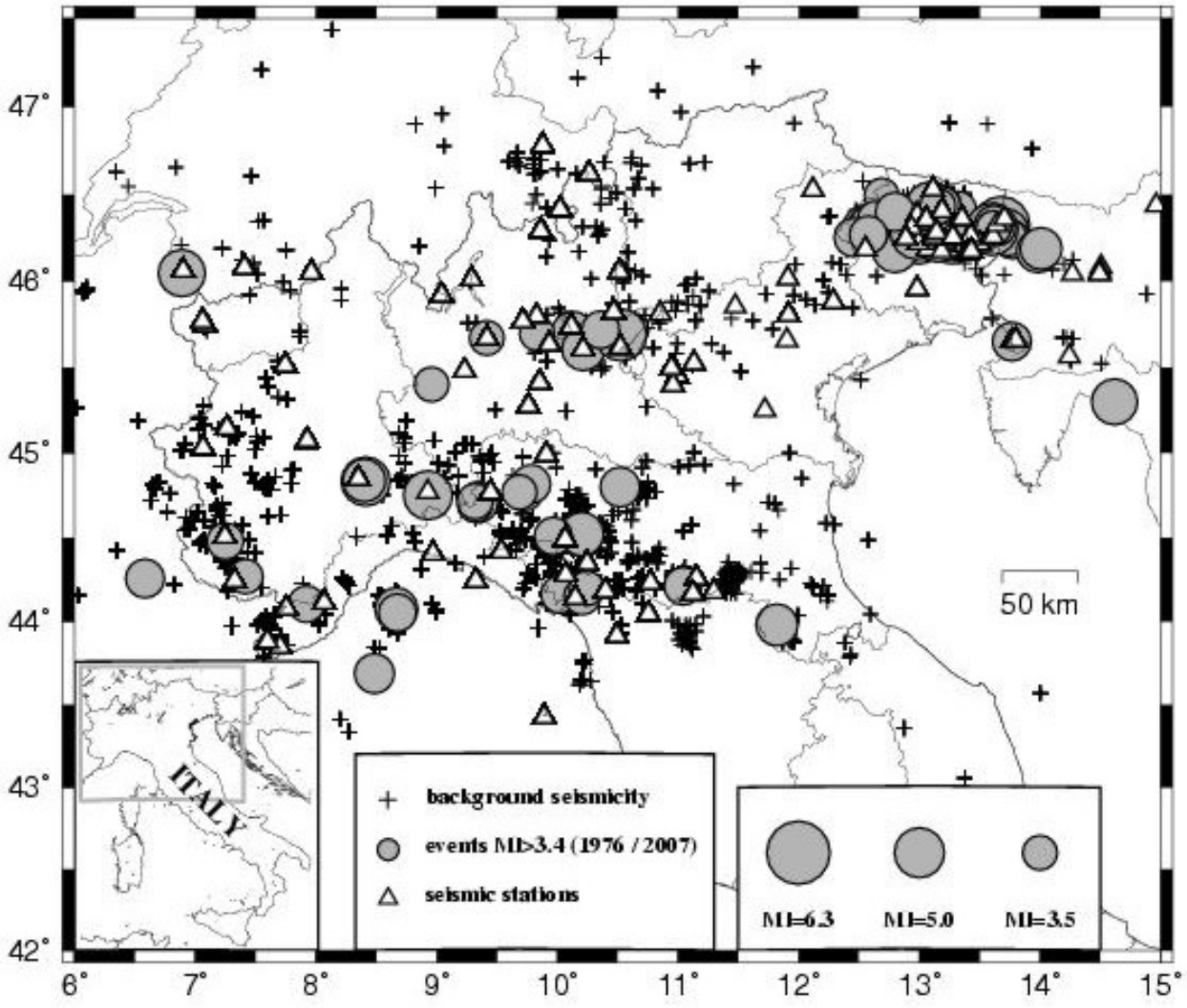
47°
46°
45°
44°
43°
42°
6°
7°
8°
9°
10°
11°
12°
13°
14°
15°
50 km
ITALY
background seismicity
events Ml>3.4 (1976 / 2007)
seismic stations
Ml=6.3
Ml=5.0
Ml=3.5

Figure 1

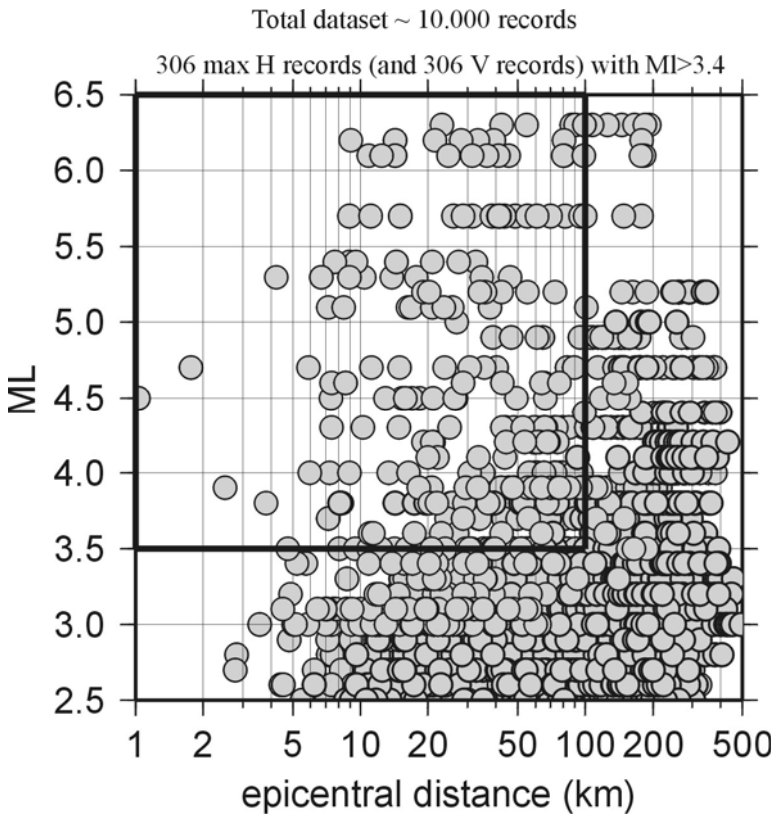
Total dataset ~ 10.000 records
306 max H records (and 306 V records) with Ml>3.4
ML
6.5
6.0
5.5
5.0
4.5
4.0
3.5
3.0
2.5
1
2
5
10
20
50
100
200
500
epicentral distance (km)

Figure 2

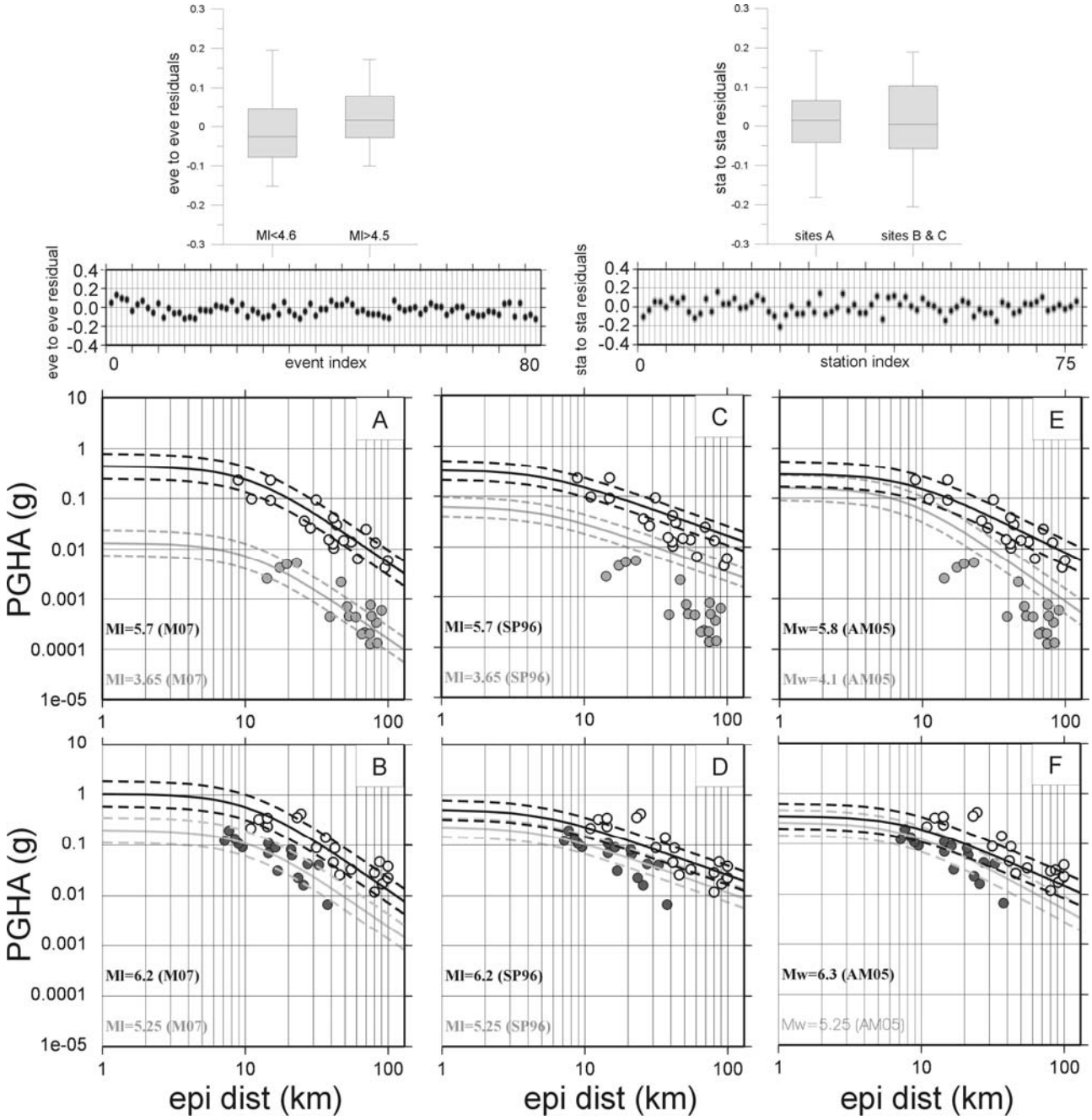
eve to eve residuals
Ml<4.6
Ml>4.5
sta to sta residuals
sites A
sites B & C
eve to eve residual
event index
sta to sta residuals
station index
A
B
C
D
E
F
PGHA (g)
Ml=5.7 (M07)
Ml=3.65 (M07)
Ml=6.2 (M07)
Ml=5.25 (M07)
Ml=5.7 (SP96)
Ml=3.65 (SP96)
Ml=6.2 (SP96)
Ml=5.25 (SP96)
Mw=5.8 (AM05)
Mw=4.1 (AM05)
Mw=6.3 (AM05)
Mw=5.25 (AM05)
epi dist (km)

Figure 3

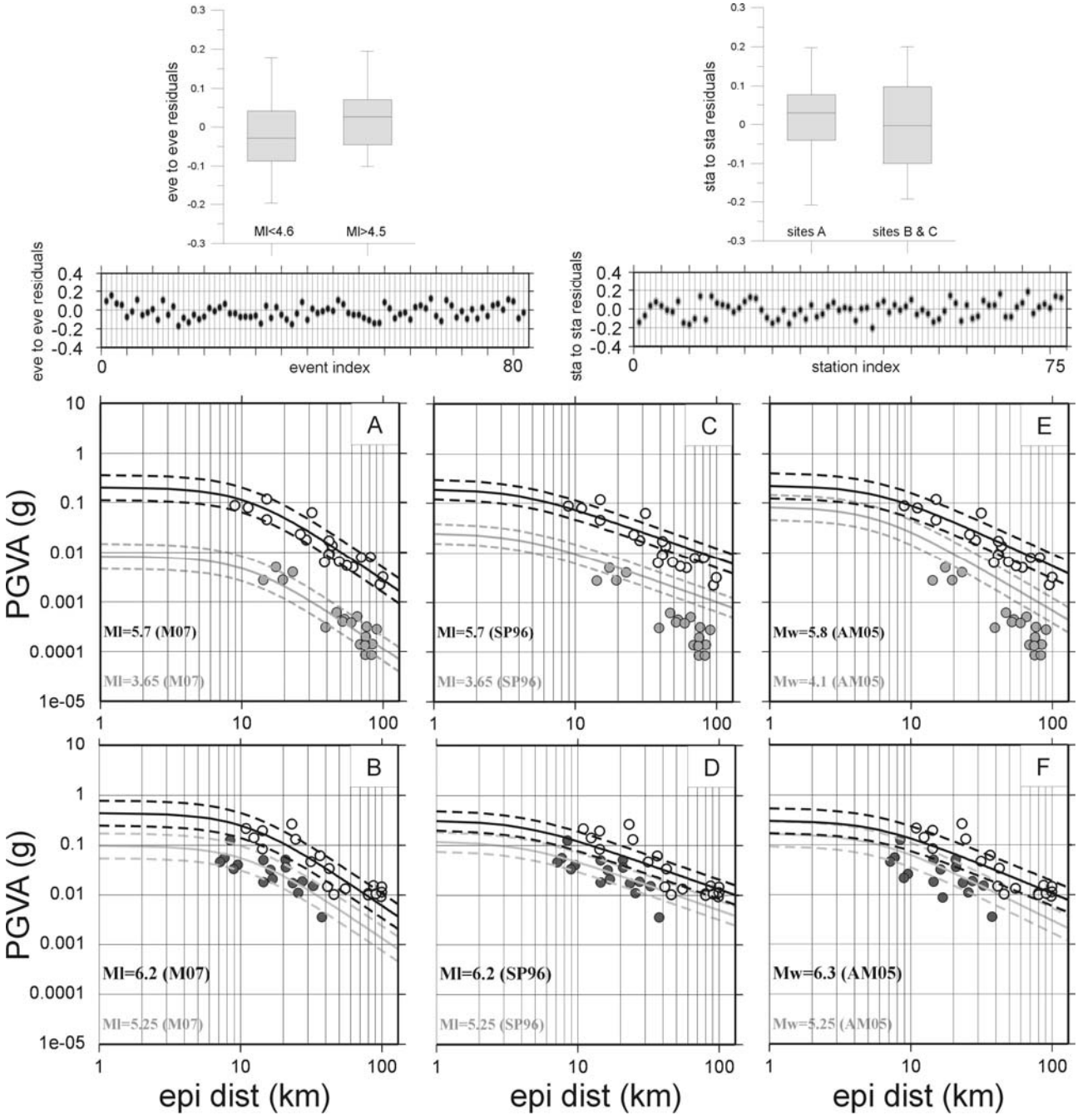
eve to eve residuals
Ml<4.6
Ml>4.5
sta to sta residuals
sites A
sites B & C
event index
station index
PGVA (g)
epi dist (km)
A
B
C
D
E
F
Ml=5.7 (M07)
Ml=3.65 (M07)
Ml=6.2 (M07)
Ml=5.25 (M07)
Ml=5.7 (SP96)
Ml=3.65 (SP96)
Ml=6.2 (SP96)
Ml=5.25 (SP96)
Mw=5.8 (AM05)
Mw=4.1 (AM05)
Mw=6.3 (AM05)
Mw=5.25 (AM05)

Figure 4

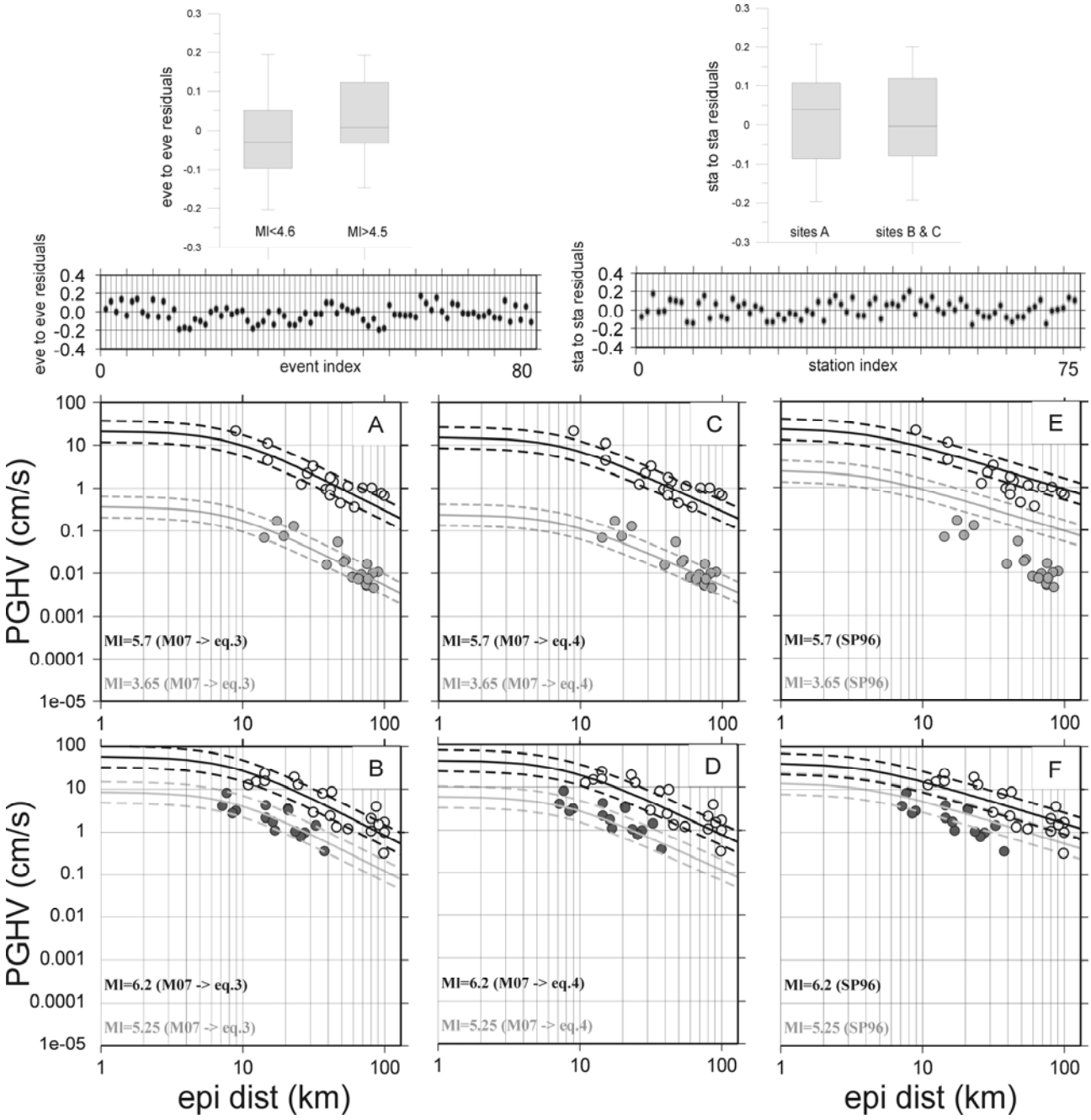
eve to eve residuals
Ml<4.6
Ml>4.5
sta to sta residuals
sites A
sites B & C
event index
station index
PGHV (cm/s)
epi dist (km)
A
B
C
D
E
F
Ml=5.7 (M07 -> eq.3)
Ml=3.65 (M07 -> eq.3)
Ml=6.2 (M07 -> eq.3)
Ml=5.25 (M07 -> eq.3)
Ml=5.7 (M07 -> eq.4)
Ml=3.65 (M07 -> eq.4)
Ml=6.2 (M07 -> eq.4)
Ml=5.25 (M07 -> eq.4)
Ml=5.7 (SP96)
Ml=3.65 (SP96)
Ml=6.2 (SP96)
Ml=5.25 (SP96)

Figure 5

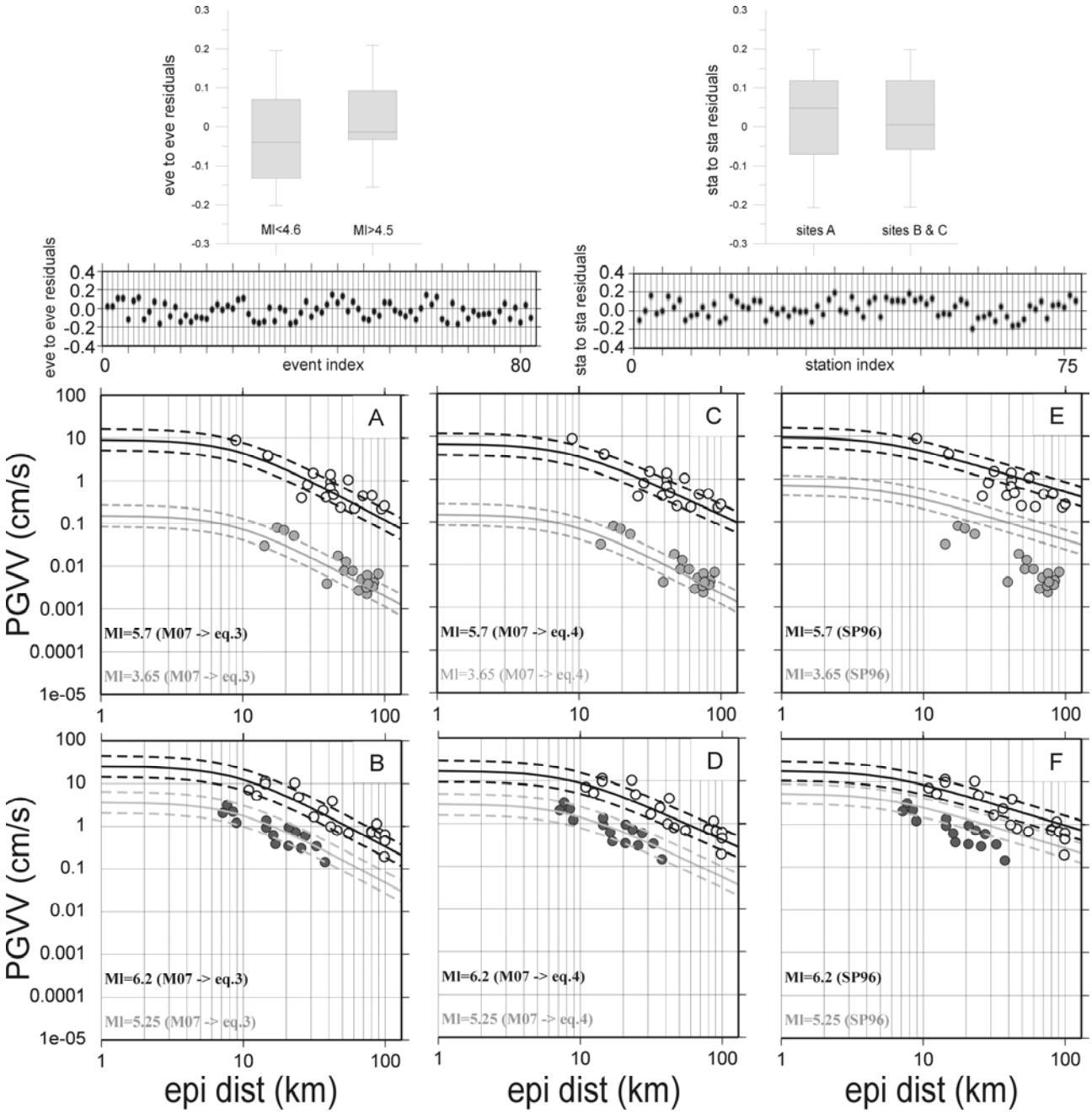
eve to eve residuals
Ml<4.6
Ml>4.5
sta to sta residuals
sites A
sites B & C
eve to eve residuals
event index
sta to sta residuals
station index
PGVV (cm/s)
A
C
E
Ml=5.7 (M07 -> eq.3)
Ml=3.65 (M07 -> eq.3)
Ml=5.7 (M07 -> eq.4)
Ml=3.65 (M07 -> eq.4)
Ml=5.7 (SP96)
Ml=3.65 (SP96)
B
D
F
Ml=6.2 (M07 -> eq.3)
Ml=5.25 (M07 -> eq.3)
Ml=6.2 (M07 -> eq.4)
Ml=5.25 (M07 -> eq.4)
Ml=6.2 (SP96)
Ml=5.25 (SP96)
epi dist (km)

Figure 6

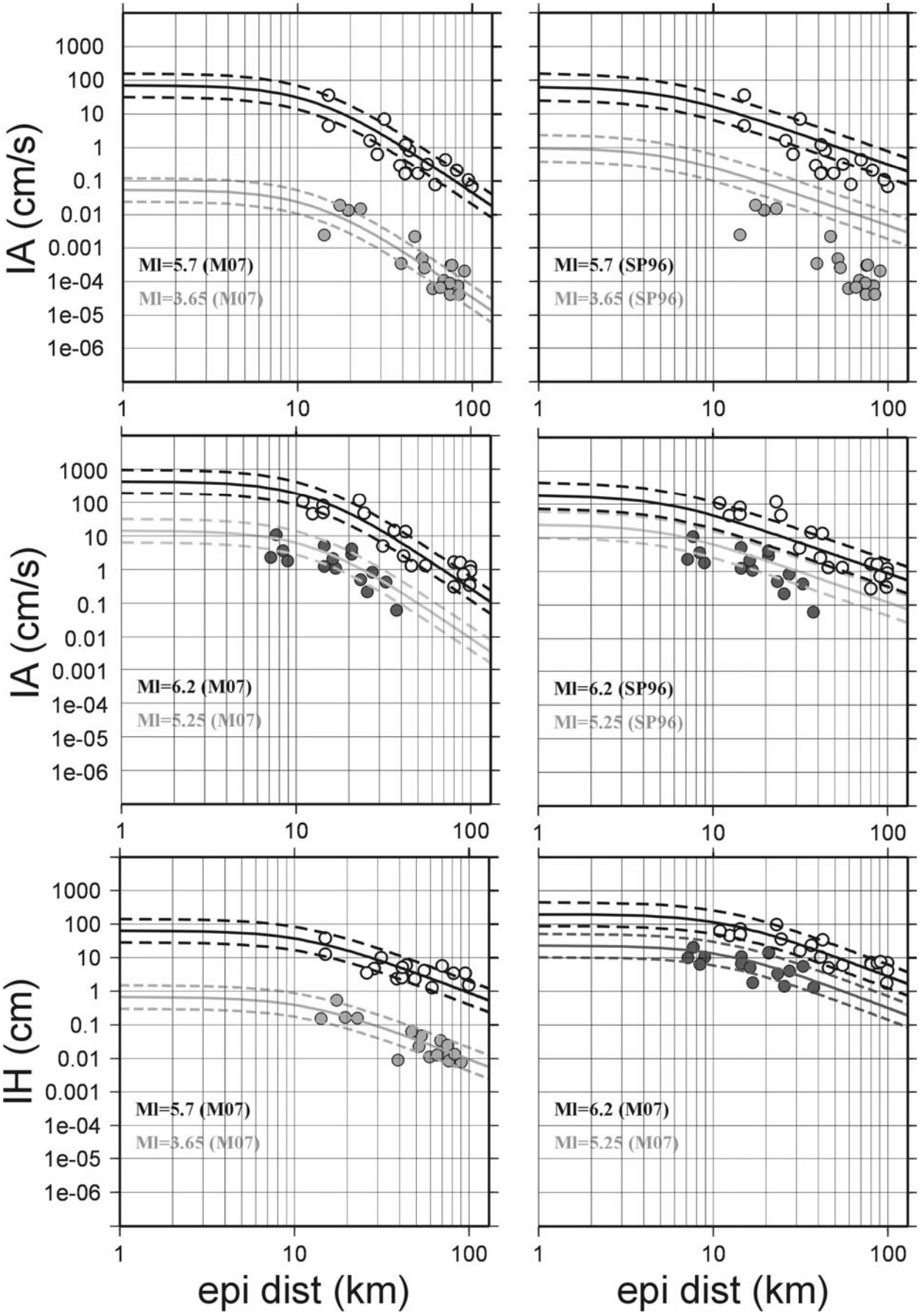
IA (cm/s)
IH (cm)
epi dist (km)
epi dist (km)
Ml=5.7 (M07)
Ml=3.65 (M07)
Ml=5.7 (SP96)
Ml=3.65 (SP96)
Ml=6.2 (M07)
Ml=5.25 (M07)
Ml=6.2 (SP96)
Ml=5.25 (SP96)
Ml=5.7 (M07)
Ml=3.65 (M07)
Ml=6.2 (M07)
Ml=5.25 (M07)

Figure 7

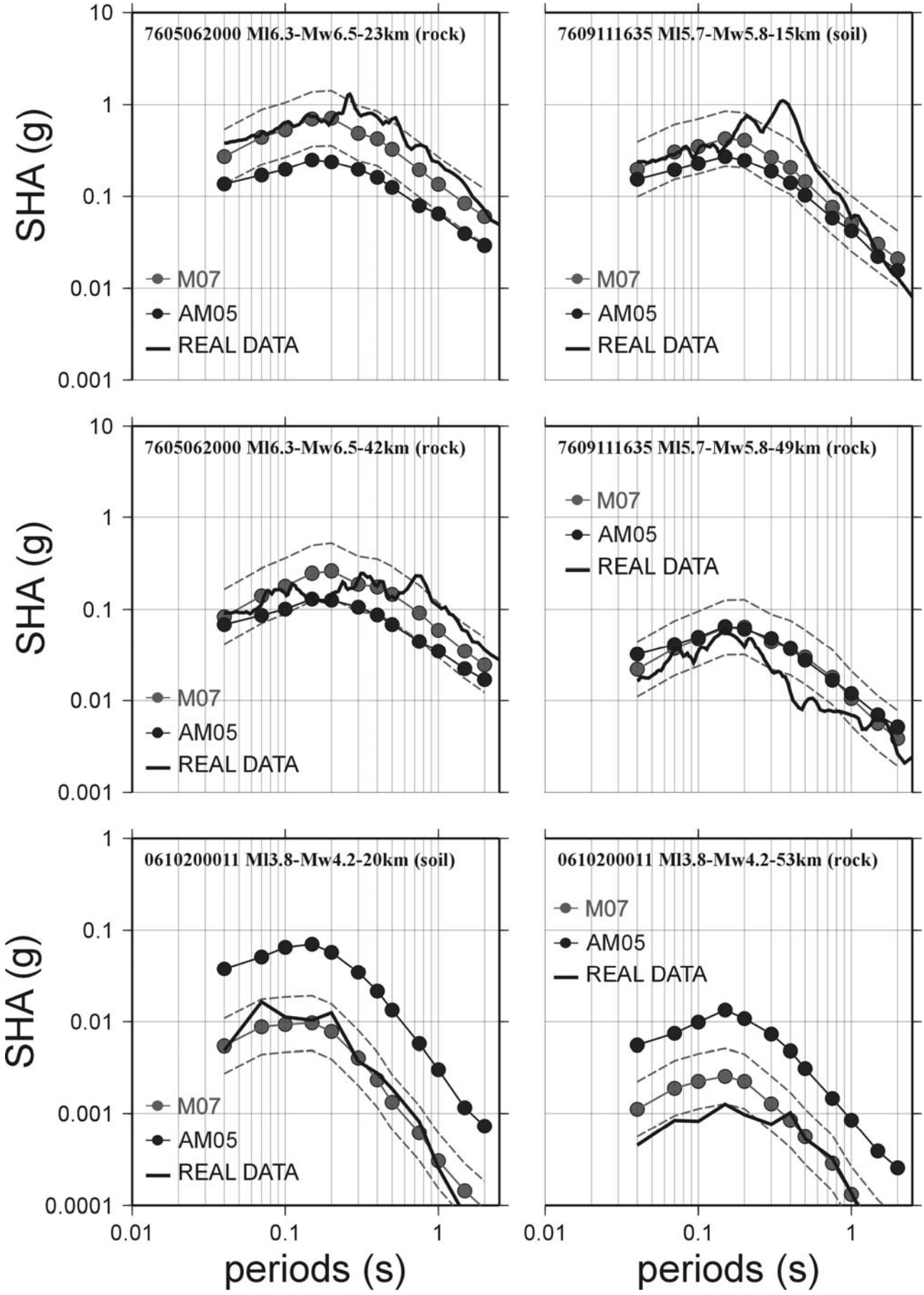
7605062000 Ml6.3-Mw6.5-23km (rock)
7609111635 Ml5.7-Mw5.8-15km (soil)
7605062000 Ml6.3-Mw6.5-42km (rock)
7609111635 Ml5.7-Mw5.8-49km (rock)
0610200011 Ml3.8-Mw4.2-20km (soil)
0610200011 Ml3.8-Mw4.2-53km (rock)
M07
AM05
REAL DATA
SHA (g)
periods (s)
10
1
0.1
0.01
0.001
0.0001

Figure 8

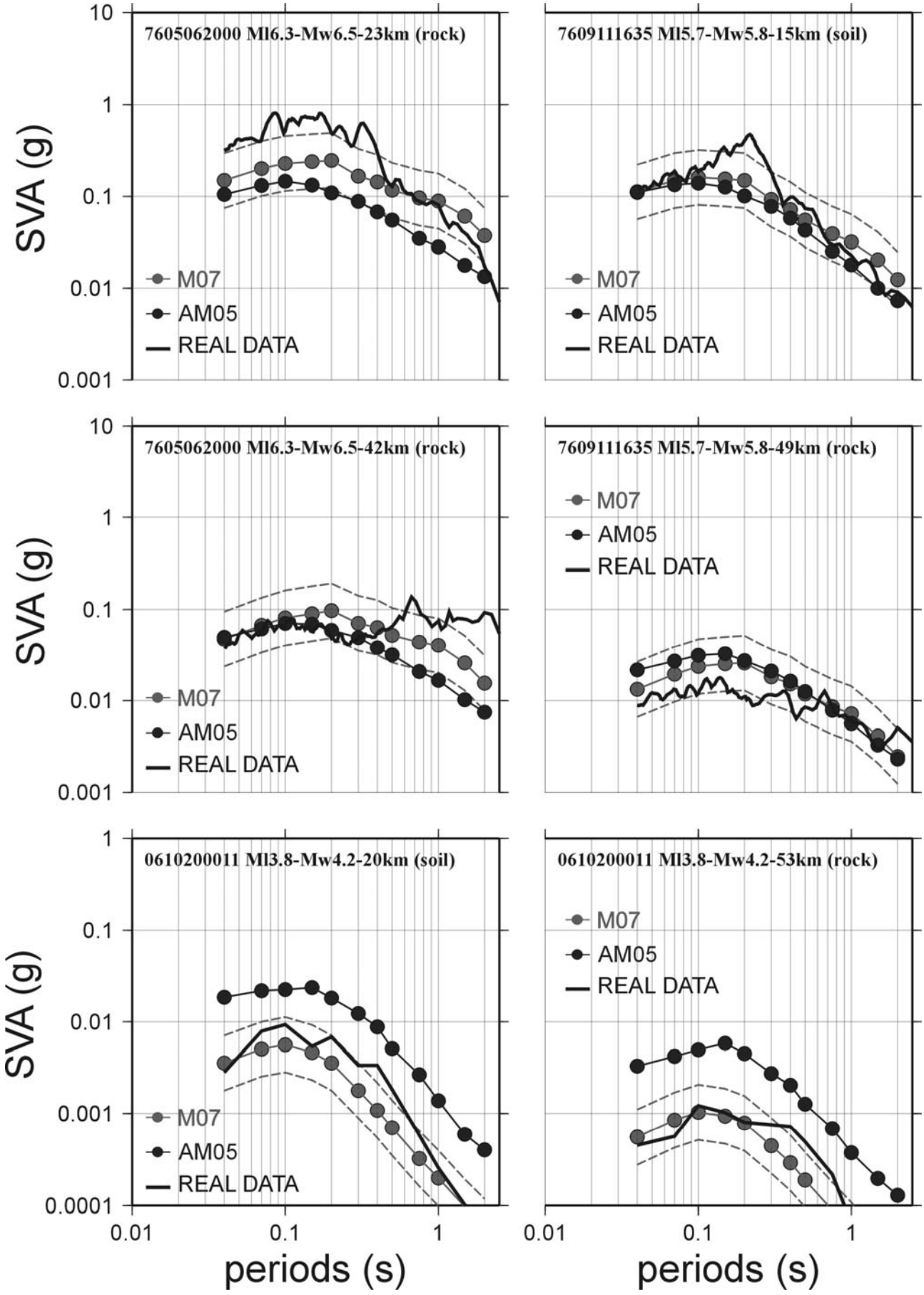
7605062000 Ml6.3-Mw6.5-23km (rock)
7609111635 Ml5.7-Mw5.8-15km (soil)
7605062000 Ml6.3-Mw6.5-42km (rock)
7609111635 Ml5.7-Mw5.8-49km (rock)
0610200011 Ml3.8-Mw4.2-20km (soil)
0610200011 Ml3.8-Mw4.2-53km (rock)
M07
AM05
REAL DATA
SVA (g)
periods (s)
10
1
0.1
0.01
0.001
0.0001

Figure 9

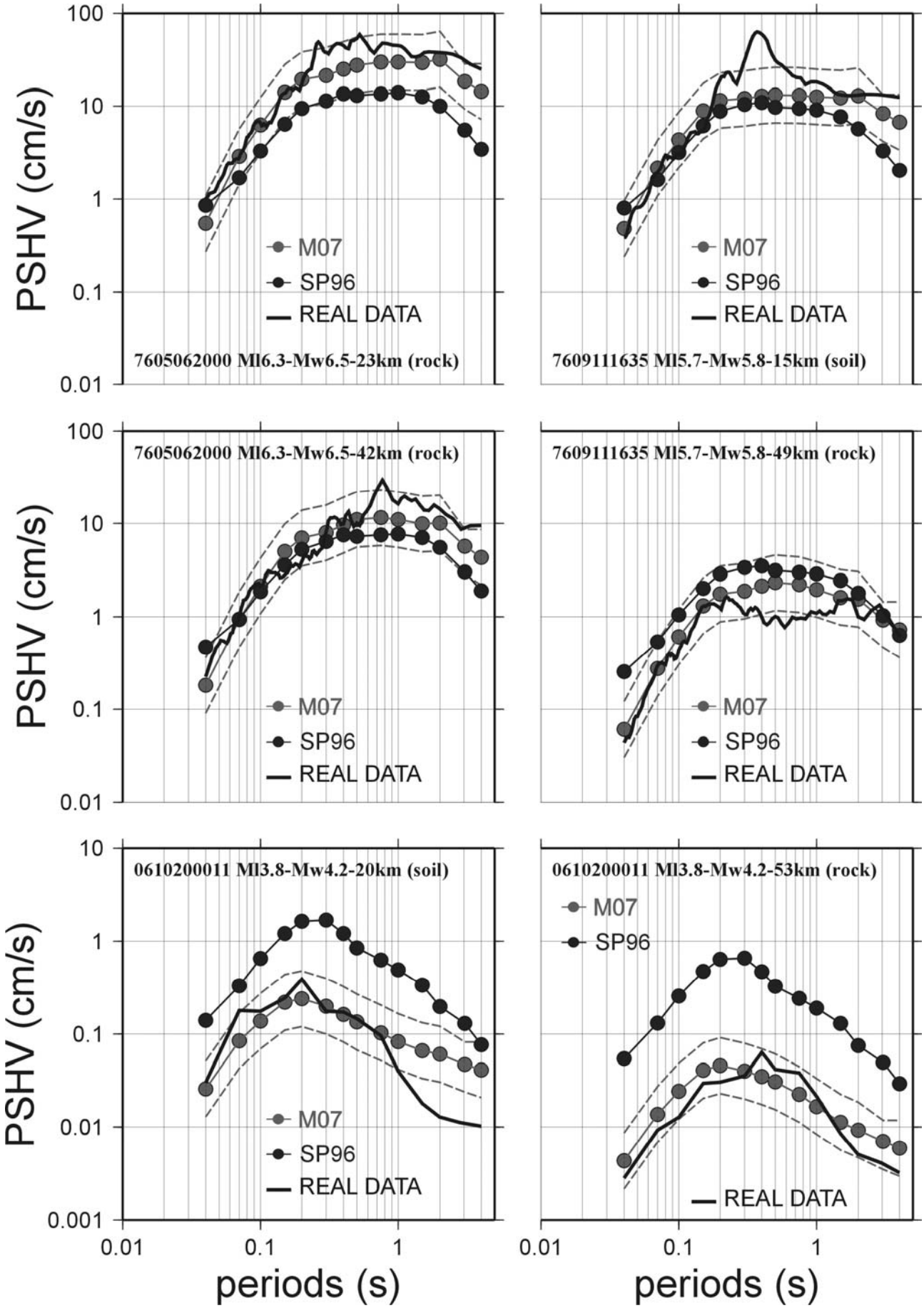
PSHV (cm/s)
periods (s)
M07
SP96
REAL DATA
7605062000 Ml6.3-Mw6.5-23km (rock)
7609111635 Ml5.7-Mw5.8-15km (soil)
7605062000 Ml6.3-Mw6.5-42km (rock)
7609111635 Ml5.7-Mw5.8-49km (rock)
0610200011 Ml3.8-Mw4.2-20km (soil)
0610200011 Ml3.8-Mw4.2-53km (rock)

Figure 10

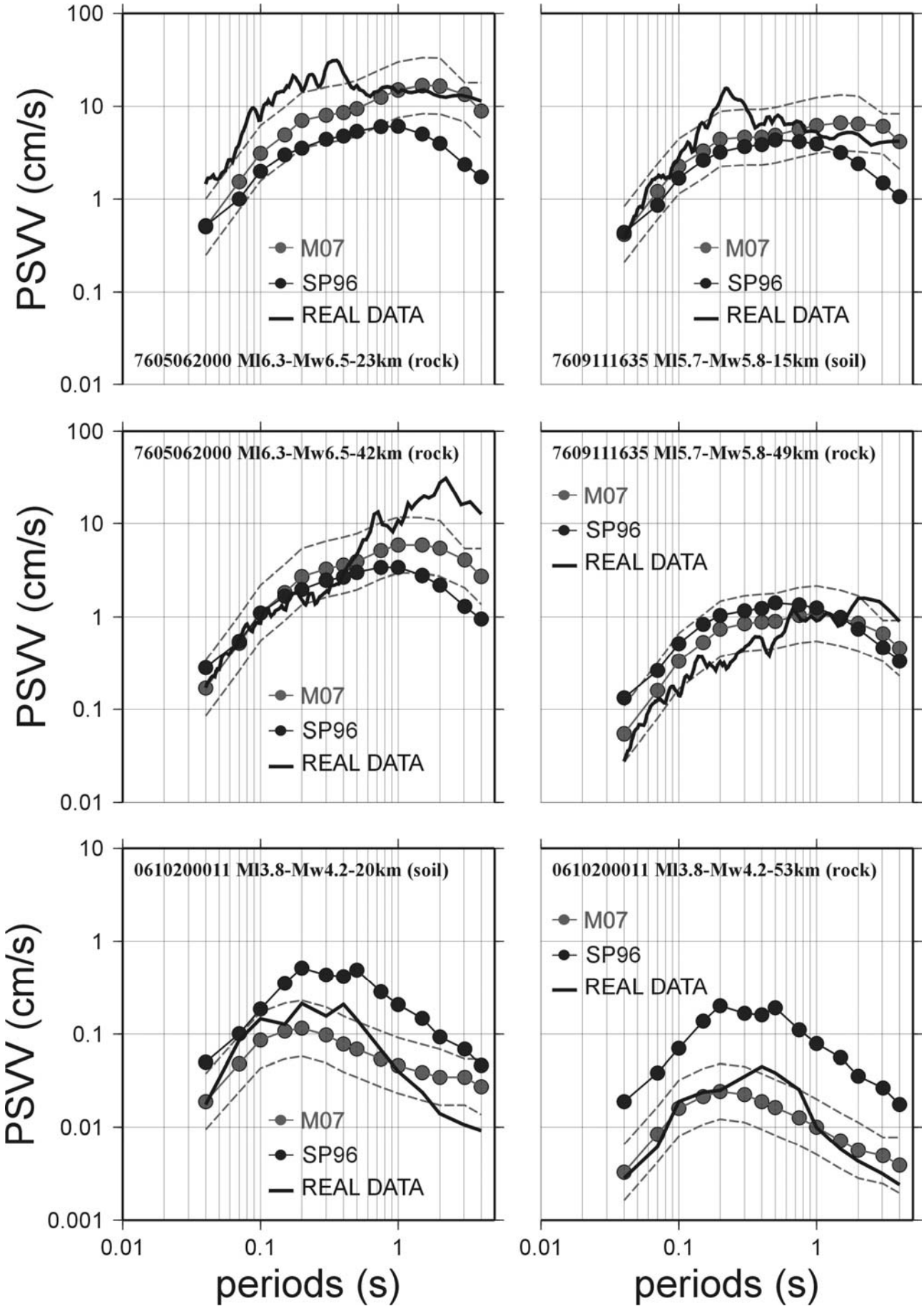
PSVV (cm/s)
periods (s)
M07
SP96
REAL DATA
7605062000 Ml6.3-Mw6.5-23km (rock)
7609111635 Ml5.7-Mw5.8-15km (soil)
7605062000 Ml6.3-Mw6.5-42km (rock)
7609111635 Ml5.7-Mw5.8-49km (rock)
0610200011 Ml3.8-Mw4.2-20km (soil)
0610200011 Ml3.8-Mw4.2-53km (rock)

Figure 11

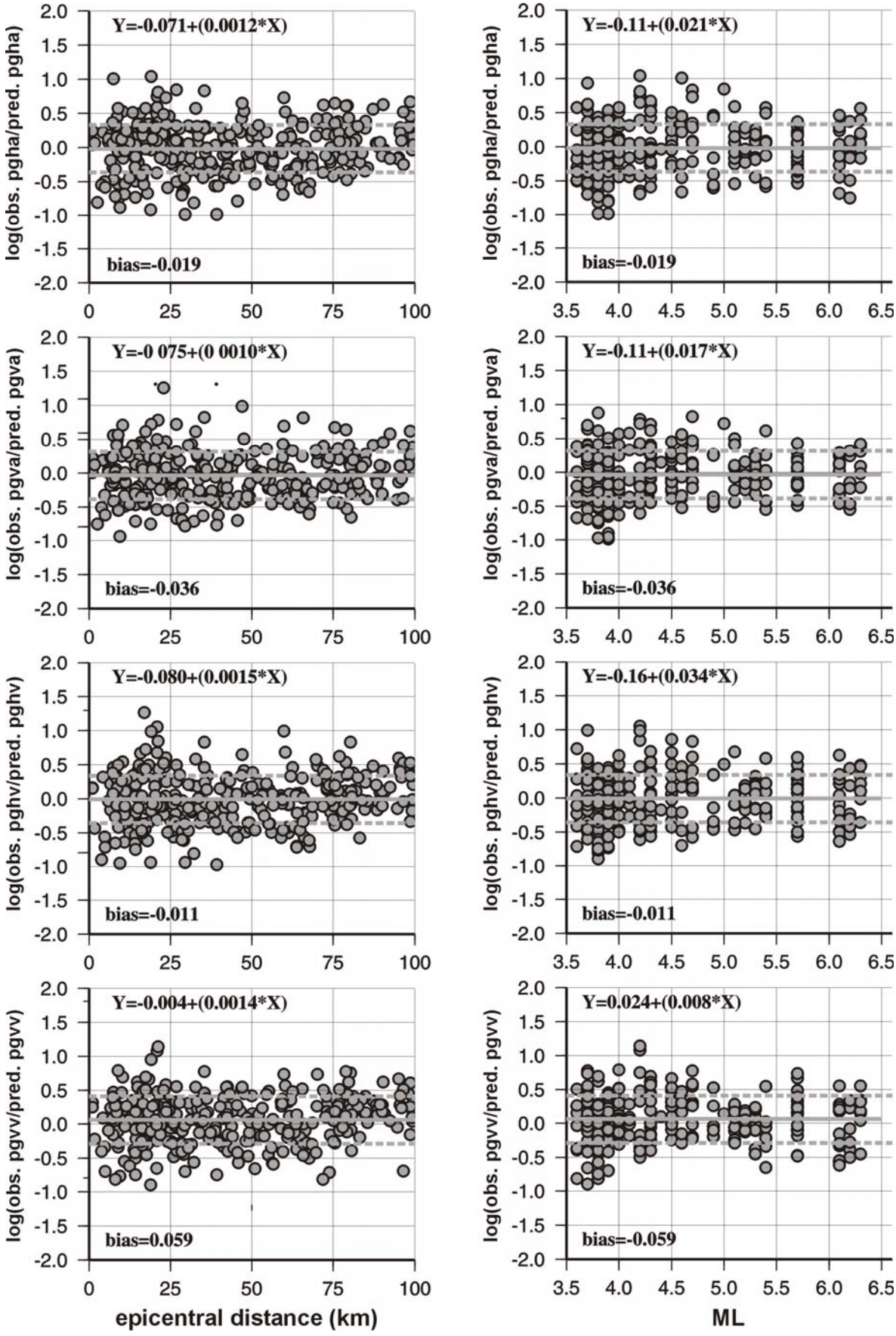
Y=-0.071+(0.0012*X)
log(obs. pgha/pred. pgha)
bias=-0.019
Y=-0.11+(0.021*X)
log(obs. pgha/pred. pgha)
bias=-0.019
Y=-0 075+(0 0010*X)
log(obs. pgva/pred. pgva)
bias=-0.036
Y=-0.11+(0.017*X)
log(obs. pgva/pred. pgva)
bias=-0.036
Y=-0.080+(0.0015*X)
log(obs. pghv/pred. pghv)
bias=-0.011
Y=-0.16+(0.034*X)
log(obs. pghv/pred. pghv)
bias=-0.011
Y=-0.004+(0.0014*X)
log(obs. pgvv/pred. pgvv)
bias=0.059
Y=0.024+(0.008*X)
log(obs. pgvv/pred. pgvv)
bias=-0.059
epicentral distance (km)
ML

Figure 12

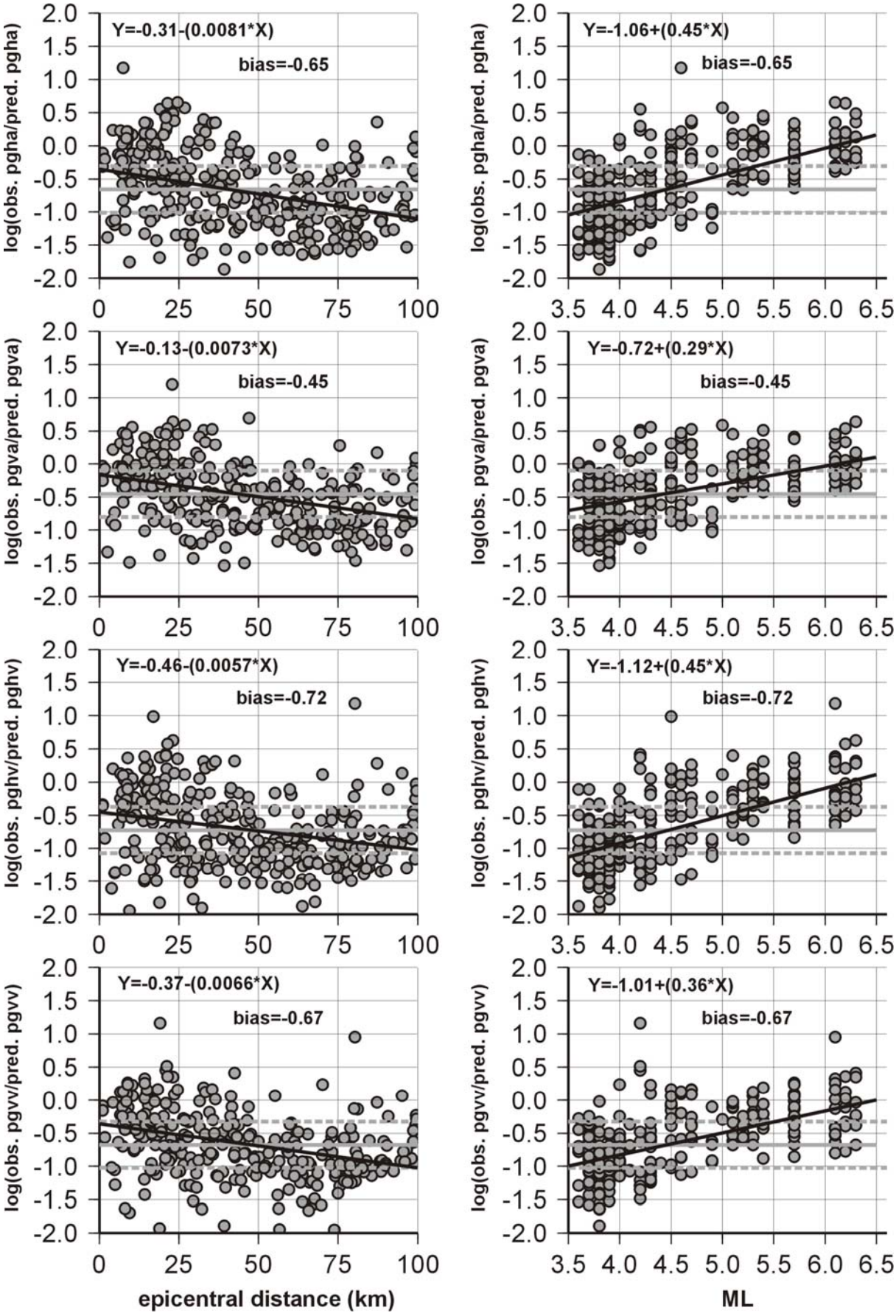
Y=-0.31-(0.0081*X)
bias=-0.65
log(obs. pgha/pred. pgha)
Y=-1.06+(0.45*X)
bias=-0.65
log(obs. pgha/pred. pgha)
Y=-0.13-(0.0073*X)
bias=-0.45
log(obs. pgva/pred. pgva)
Y=-0.72+(0.29*X)
bias=-0.45
log(obs. pgva/pred. pgva)
Y=-0.46-(0.0057*X)
bias=-0.72
log(obs. pghv/pred. pghv)
Y=-1.12+(0.45*X)
bias=-0.72
log(obs. pghv/pred. pghv)
Y=-0.37-(0.0066*X)
bias=-0.67
log(obs. pgvv/pred. pgvv)
Y=-1.01+(0.36*X)
bias=-0.67
log(obs. pgvv/pred. pgvv)
epicentral distance (km)
ML

Figure 13

Code	Name	Lat [°]	Long [°]	Elevation [m]	Sensor	Owner	EC8 Soil Class
BAG3	Bagolino	45.822	10.466	807	LE-3D5s/Episensor	INGV-MI	A
BAG2	Bagolino	45.822	10.466	807	LE-3D5s	INGV-MI	A
MAL3	Malenco	46.291	9.863	2030	LE-3D5s/Episensor	INGV-MI	A
MAL2	Malenco	46.291	9.863	2030	LE-3D5s	INGV-MI	A
MER2	Merate	45.672	9.418	350	Trillium	INGV-MI	B
MAR2	Marone	45.739	10.117	600	Trillium	INGV-MI	A
ASO2	Asolo	45.804	11.918	221	LE-3D1s/Episensor	INGV-MI	A
NEGR	Negrar	45.497	10.948	167	LE-3D5s/Episensor	INGV-MI	A
CTLE	Castelleone	45.276	9.762	66	Trillium/Episensor	INGV-MI	C
COR2	Cortemaggiore	44.990	9.907	52	Trillium	INGV-MI	C
MILA	Milano	45.480	9.232	125	Trillium/Episensor	INGV-MI	B
BOB	Bobbio	44.767	9.447	910	Trillium/Episensor	INGV-CNT	A
FNVD	Fontana Vidola	44.167	11.122	950	Trillium/Episensor	INGV-CNT	A
MABI	Malga Bissina	46.054	10.514	1853	Trillium/Episensor	INGV-CNT	A
SALO	Salò	45.607	10.525	90	Trillium/Episensor	INGV-CNT	A
MDI	Monte di Nese	45.770	9.716	954	Trillium/Episensor	INGV-CNT	A
EMV	Vieux Emosson	46.063	6.898	2210	STS-2/Episensor	SDSNet	A
DIX	Grand Dixence	46.080	7.404	2400	STS-2/Episensor	SDSNet	A
MMK	Mattmark	46.051	7.965	2200	STS-2/Episensor	SDSNet	A
BACM	Baccana	44.278	10.072	490	LE-3D5s	UNI-GE	A
FENM	Fenestrelle	45.030	7.062	1000	CMG03	UNI-GE	A
GENL	Genova	44.405	8.969	80	CMG40	UNI-GE	A
GRAM	Graiana	44.491	10.065	871	LE-3D5s	UNI-GE	A
MAIM	Mastiano	43.914	10.491	290	LE-3D5s	UNI-GE	B
MONE	Monesi	44.079	7.755	1320	CMG40	UNI-GE	A
NEGI	Negi	43.847	7.704	640	CMG40	UNI-GE	B
POPM	Popiglio	44.045	10.757	300	LE-3D5s	UNI-GE	A
RONM	Rocchetta Nervina	43.881	7.598	300	LE-3D5s	UNI-GE	A
RORM	Roccarossa	44.112	8.066	390	LE-3D5s	UNI-GE	A
ROTM	Rocchetta Tanaro	44.849	8.352	221	LE-3D5s	UNI-GE	B
SARM	Sassorosso	44.184	10.401	1040	LE-3D5s	UNI-GE	A
SCUM	Scurtabo'	44.416	9.537	710	LE-3D5s	UNI-GE	A
SESM	Sestola	44.231	10.773	900	LE-3D5s	UNI-GE	A
STV2	S.Anna di Valdieri	44.245	7.326	930	CMG40	UNI-GE	A
TRAV	Traversella	45.512	7.747	990	CMG40	UNI-GE	A
VALM	Valbona	44.348	10.247	790	LE-3D5s	UNI-GE	B
VINM	Vinca	44.141	10.152	710	LE-3D5s	UNI-GE	A
BARC	Barcis	46.187	12.554	420	SMA-1	SSN-DPC*	C
BRFA	Breginj	46.264	13.429	555	CMG40	ARSO	B
BUIA	Buia	46.222	13.090	250	SMA-1	SSN-DPC*	C
CARC	TS - Carciotti	45.653	13.770	2	Episensor	UNI-TS	C
CASS	Cassacco	46.175	13.188	175	FBA23	UNI-TS	C
CESC	Cesclans	46.356	13.058	355	FBA23	UNI-TS	B
CODR	Codroipo	45.959	12.984	30	SMA-1	SSN-DPC*	B
CONE	Conegliano	45.883	12.288	65	SMA-1	SSN-DPC*	B
COTT	Cortina	46.525	12.118	1550	SMA-1	SSN-DPC*	B

* Stations of italian civil defence (Dipartimento di Protezione Civile) that were managed by ENEL in 1976

Table 1a

Code	Name	Lat [°]	Long [°]	Elevation [m]	Sensor	Owner	EU8 Soil Class
DREZ	Dreznica	46.259	13.612	541	FBA23	ARSO	A
DST2	TS - DST	45.659	13.801	80	STS-2/Episensor	UNI-TS	A
FELT	Feltre	46.019	11.912	320	SMA-1	SSN-DPC*	A
FORG	Forgaria	46.221	12.997	205	SMA-1	SSN-DPC*	B
GEDE	Gemona 1	46.254	13.124	232	Episensor	UNI-TS	C
GEPF	Gemona 2	46.277	13.140	255	STS2 - Episensor	UNI-TS	A
GESC	Gemona 3	46.283	13.142	325	Episensor	UNI-TS	B
GETM	Gemona 4	46.267	13.115	188	SSA-1	UNI-TS	C
ILBR	Iliriska Bistrica	45.564	14.244	407	SMA-1	ARSO	A
KLLE	Klin - Lepena	46.328	13.643	420	FBA23	ARSO	A
KOBA	Kobarid	46.247	13.582	388	SMA-1	ARSO	C
LJFC	Ljubljana 1	46.044	14.494	296	SMA-1	ARSO	A
LJGO	Ljubljana 2	46.043	14.270	368	SMA-1	ARSO	A
LJIM	Ljubljana 3	46.083	14.508	357	SMA-1	ARSO	A
LJZR	Ljubljana 4	46.058	14.500	385	SMA-1	ARSO	B
MAJA	Majano	46.187	13.073	168	SMA-1	SSN-DPC*	B
MASA	Masarolis	46.177	13.432	640	Episensor	UNI-TS	B
MOGG	Moggio Udinese	46.406	13.189	387	Episensor	UNI-TS	A
PAUL	Paularo	46.530	13.116	640	Episensor	UNI-TS	A
PRAD	Pradis	46.248	12.889	520	Episensor	UNI-TS	A
ROBI	Robic	46.218	13.502	412	SMA-1	ARSO	A
SFRA	S. Francesco	46.310	12.935	375	FBA23	UNI-TS	A
SLEM	Sleme	46.438	14.966	257	SMA-1	ARSO	A
SOMP	Somplago	46.338	13.061	195	SMA-1	SSN-DPC*	A
SROC	S. Rocco	46.221	12.997	405	SMA-1	SSN-DPC*	B
STOL	Stolvizza	46.361	13.355	570	Episensor	UNI-TS	A
TARC	Tarcento	46.226	13.210	230	SMA-1	SSN-DPC*	B
TOLM	Tolmezzo	46.382	12.982	525	SMA-1	SSN-DPC*	A
TREN	Trenta	46.362	13.705	680	FBA23	ARSO	A
VALL	Valle	46.158	13.393	666	CMG-5T	UNI-TS	B
VINO	Villanova	46.256	13.281	608	CMG-3T/Episensor	UNI-TS	A

* Stations of italian civil defence (Dipartimento di Protezione Civile) that were managed by ENEL in 1976

Table 1b

Event	dd/mm/yyyy	hh:mm:ss	Lon [°]	Lat [°]	Depth[km]	Ml	Mw	rec
1	06/05/1976	20:00:12	13.253	46.292	7.0	6.3	6.5	42
2	07/05/1976	00:23:50	13.269	46.245	9.0	5.0	5.2	30
3	09/05/1976	00:53:43	13.236	46.316	10.0	4.2	4.5	18
4	10/05/1976	04:35:51	13.220	46.280	5.0	4.5	4.8	12
5	11/05/1976	22:43:59	12.985	46.258	6.0	5.3	5.4	30
6	11/06/1976	17:16:40	13.000	46.230	9.0	4.5	4.8	18
7	17/06/1976	14:28:49	12.800	46.180	15.0	4.5	4.8	12
8	11/09/1976	16:31:13	13.160	46.286	3.0	5.4	5.5	48
9	11/09/1976	16:35:00	13.175	46.277	12.0	5.7	5.8	48
10	13/09/1976	18:54:45	13.146	46.306	8.0	4.3	4.6	18
11	15/09/1976	03:15:19	13.153	46.291	5.0	6.2	6.3	42
12	15/09/1976	04:38:53	13.132	46.318	7.0	4.7	5.0	36
13	15/09/1976	09:21:18	13.119	46.318	8.0	6.1	6.1	66
14	16/09/1977	23:48:05	12.980	46.280	8.0	5.3	5.5	42
15	21/02/1994	07:31:16	13.215	46.328	5.0	3.5	4.0	12
16	22/02/1994	04:14:59	13.056	46.301	7.0	3.5	4.0	12
17	14/12/1994	03:38:17	13.305	46.279	12.6	3.8	4.2	12
18	27/01/1996	08:25:59	12.575	46.314	6.1	3.8	4.2	12
19	27/02/1996	11:13:45	12.577	46.309	9.5	4.3	4.6	18
20	13/04/1996	13:00:22	12.559	46.312	11.5	4.5	4.7	12
21	16/04/1996	18:06:51	12.570	46.321	13.9	3.8	4.2	12
22	11/07/1996	19:09:28	10.021	44.163	4.5	3.8	4.2	18
23	18/02/1997	21:42:42	10.205	44.522	57.9	4.4	4.7	12
24	24/02/1997	12:06:17	8.486	43.687	8.1	4.0	4.3	12
25	31/10/1997	04:23:43	6.586	44.257	5.3	3.9	4.3	12
26	08/11/1997	01:56:07	7.921	44.106	6.6	3.7	4.1	18
27	12/04/1998	10:55:32	13.678	46.324	15.2	5.7	5.8	66
28	12/04/1998	13:35:27	13.564	46.258	16.0	3.5	4.0	12
29	12/04/1998	22:13:48	13.612	46.314	13.9	3.7	4.1	12
30	15/04/1998	19:40:30	13.733	46.272	9.8	3.8	4.2	24
31	15/04/1998	22:42:10	13.658	46.317	11.5	3.6	4.0	12
32	06/05/1998	02:53:00	13.717	46.285	7.9	4.6	4.9	36
33	11/05/1998	23:30:48	13.719	46.271	14.6	3.7	4.1	12
34	28/05/1998	09:32:19	13.049	46.295	10.6	4.0	4.4	18
35	10/06/1998	23:32:41	13.613	46.292	13.5	3.5	4.0	12
36	30/08/1998	01:18:21	13.771	46.239	19.1	3.8	4.2	18
37	24/11/1998	13:49:32	13.738	46.253	14.7	3.7	4.1	12
38	21/03/1999	04:07:42	13.330	46.418	6.4	3.5	4.0	18
39	13/05/1999	16:06:52	13.610	46.269	11.1	3.9	4.3	12
40	19/06/1999	20:18:09	12.690	46.493	10.3	3.5	4.0	12
41	21/08/2000	17:14:28	8.413	44.832	5.0	4.9	4.9	30
42	01/02/2001	21:57:47	9.965	44.510	12.0	3.8	4.2	24
43	06/02/2001	22:28:46	8.665	44.074	9.8	4.3	4.6	18
44	03/06/2001	00:03:20	8.675	44.054	11.7	3.8	4.2	12
45	18/07/2001	22:47:10	8.401	44.837	5.2	4.3	4.6	18
46	14/02/2002	03:18:02	13.100	46.426	11.2	5.1	5.0	48
47	06/05/2002	03:24:17	12.638	46.360	12.2	3.7	4.1	12
48	30/09/2002	02:48:30	13.612	46.331	11.3	4.1	4.4	18

Table 2a

Event	dd/mm/yyyy	hh:mm:ss	Lon [°]	Lat [°]	Depth[km]	Ml	Mw	rec
49	13/11/2002	10:48:04	10.129	45.704	5.0	4.2	4.5	24
50	11/03/2003	05:57:09	13.185	46.440	16.0	3.8	4.2	18
51	11/04/2003	09:26:58	8.929	44.752	18.6	4.8	5.0	30
52	18/04/2003	01:17:41	12.958	46.348	11.0	3.5	4.0	12
53	30/08/2003	09:10:51	12.800	46.400	9.0	3.9	4.3	18
54	01/09/2003	19:28:11	7.420	44.269	1.9	3.5	4.0	18
55	12/07/2004	13:03:35	13.604	46.301	6.0	5.2	5.4	30
56	12/07/2004	16:26:59	13.654	46.306	5.0	3.5	4.0	12
57	14/07/2004	04:37:37	13.615	46.327	5.0	3.8	4.2	18
58	27/08/2004	21:47:36	10.208	44.149	5.0	3.7	4.1	18
59	29/08/2004	00:04:39	12.457	46.253	5.0	3.9	4.3	24
60	14/09/2004	18:09:25	14.617	45.300	10.0	4.6	4.9	30
61	07/10/2004	19:21:08	13.154	46.434	5.0	3.7	4.1	12
62	24/11/2004	22:59:39	10.524	45.689	5.0	5.2	5.0	18
63	14/01/2005	07:58:12	13.986	46.174	16.0	4.3	4.6	30
64	14/01/2005	08:05:19	14.010	46.190	10.0	4.3	4.6	24
65	25/03/2005	23:19:28	7.250	44.478	10.9	3.7	4.1	24
66	18/04/2005	10:59:18	9.348	44.724	7.8	3.7	4.1	30
67	19/04/2005	07:42:01	9.724	44.770	25.2	3.8	4.2	24
68	19/04/2005	08:27:39	9.687	44.769	25.6	3.5	4.0	12
69	24/04/2005	18:33:59	13.770	45.653	5.0	3.9	4.3	18
70	30/04/2005	08:10:25	9.317	44.694	8.7	3.5	4.0	12
71	05/06/2005	04:18:46	9.321	44.713	6.6	3.6	4.0	18
72	08/09/2005	11:27:18	6.890	46.048	6.7	4.5	4.6	24
73	20/11/2005	10:48:58	9.958	45.403	34.5	3.5	4.0	48
74	27/03/2006	08:04:46	11.040	44.210	54.3	3.8	4.2	12
75	16/04/2006	21:15:03	11.820	43.980	6.0	4.3	4.6	24
76	02/09/2006	01:21:29	7.592	43.832	10.0	3.5	4.0	30
77	20/10/2006	00:11:58	10.360	45.720	5.0	3.8	4.2	60
78	26/02/2007	05:50:43	12.580	46.270	7.1	3.8	4.1	24
79	26/02/2007	14:16:38	12.569	46.271	7.4	3.5	4.0	30
80	23/03/2007	05:01:39	9.844	45.969	8.6	3.5	4.0	24
81	19/05/2007	16:19:41	10.586	47.035	3.0	3.5	4.0	18
82	09/05/2007	06:03:49	10.520	44.800	4.0	4.0	4.2	24

Table 2b

Ml (eq. 3)

Y (eq.1)	a	b	c	d	s1	s2	σsta	σeve	σrec	σ tot	unit
PGHA	-2.66	0.76	-1.97	10.72	0	0.13		0.09	0.27	0.28	g
PGHA	-2.66	0.76	-1.97	10.72	0	0.13	0.09		0.28	0.29	g
PGVA	-2.59	0.69	-1.95	11.16	0	0.12		0.09	0.26	0.28	g
PGVA	-2.59	0.69	-1.95	11.16	0	0.12	0.08		0.26	0.27	g
PGHV	-2.15	0.88	-1.69	8.15	0	0.19		0.08	0.27	0.28	cm/s
PGHV	-2.15	0.88	-1.69	8.15	0	0.19	0.08		0.26	0.27	cm/s
PGVV	-2.43	0.89	-1.78	8.77	0	0.03		0.09	0.27	0.28	cm/s
PGVV	-2.43	0.89	-1.78	8.77	0	0.03	0.09		0.28	0.29	cm/s
Ia	-3.07	1.56	-3.58	12.81	0	0.46		0.11	0.31	0.33	cm/s
Ia	-3.07	1.56	-3.58	12.81	0	0.46	0.10		0.30	0.32	cm/s
Ih	-1.73	0.99	-1.98	11.62	0	0.22		0.11	0.27	0.29	cm
Ih	-1.73	0.99	-1.98	11.62	0	0.22	0.09		0.28	0.29	cm
DV	-0.83	0.11	0.54	16.29	0	0.03		0.06	0.15	0.16	sec
DV	-0.83	0.11	0.54	16.29	0	0.03	0.05		0.16	0.17	sec

Table 3

SHA - Ml (eq. 3)

T (s)	a	b	c	d	s1	s2	σsta	σeve	σrec	σ tot	unit
0,040	-1.86	0.72	-2.29	12.31	0	0.13		0.11	0.25	0.27	g
0,040	-1.86	0.72	-2.29	12.31	0	0.13	0.10		0.25	0.27	g
0,070	-1.57	0.72	-2.32	14.16	0	0.15		0.10	0.25	0.27	g
0,070	-1.57	0.72	-2.32	14.16	0	0.15	0.11		0.25	0.27	g
0,100	-1.91	0.74	-2.13	12.95	0	0.20		0.10	0.26	0.28	g
0,100	-1.91	0.74	-2.13	12.95	0	0.20	0.08		0.26	0.27	g
0,150	-2.17	0.78	-2.04	13.01	0	0.24		0.09	0.25	0.27	g
0,150	-2.17	0.78	-2.04	13.01	0	0.24	0.09		0.25	0.27	g
0,200	-2.60	0.82	-1.92	11.93	0	0.26		0.09	0.27	0.28	g
0,200	-2.60	0.82	-1.92	11.93	0	0.26	0.09		0.27	0.28	g
0,300	-3.38	0.87	-1.73	9.18	0	0.25		0.10	0.25	0.27	g
0,300	-3.38	0.87	-1.73	9.18	0	0.25	0.07		0.26	0.27	g
0,400	-4.12	0.94	-1.57	7.38	0	0.25		0.10	0.26	0.28	g
0,400	-4.12	0.94	-1.57	7.38	0	0.25	0.07		0.27	0.28	g
0,500	-4.78	0.99	-1.41	6.10	0	0.22		0.11	0.26	0.28	g
0,500	-4.78	0.99	-1.41	6.10	0	0.22	0.10		0.27	0.29	g
0,750	-5.31	1.03	-1.36	8.52	0	-0.26		0.11	0.29	0.31	g
0,750	-5.31	1.03	-1.36	8.52	0	-0.26	0.08		0.31	0.32	g
1,000	-5.68	1.09	-1.48	8.64	0	0.24		0.11	0.26	0.28	g
1,000	-5.68	1.09	-1.48	8.64	0	0.24	0.09		0.29	0.30	g
1,490	-6.03	1.14	-1.60	9.10	0	0.27		0.09	0.25	0.27	g
1,490	-6.03	1.14	-1.60	9.10	0	0.27	0.10		0.25	0.27	g
2,000	-6.22	1.16	-1.65	10.02	0	0.26		0.11	0.24	0.26	g
2,000	-6.22	1.16	-1.65	10.02	0	0.26	0.10		0.26	0.28	g

Table 4

SVA - MI (eq. 3)

T (s)	a	b	c	d	s1	s2	σsta	σeve	σrec	σ tot	unit
0,040	-2.10	0.69	-2.18	11.60	0	0.06		0.11	0.26	0.28	g
0,040	-2.10	0.69	-2.18	11.60	0	0.06	0.09		0.25	0.27	g
0,070	-2.05	0.68	-2.08	11.44	0	0.05		0.08	0.27	0.28	g
0,070	-2.05	0.68	-2.08	11.44	0	0.05	0.10		0.26	0.28	g
0,100	-2.01	0.68	-2.05	13.03	0	0.07		0.10	0.28	0.30	g
0,100	-2.01	0.68	-2.05	13.03	0	0.07	0.10		0.26	0.28	g
0,150	-2.45	0.72	-1.91	12.51	0	0.11		0.09	0.26	0.28	g
0,150	-2.45	0.72	-1.91	12.51	0	0.11	0.08		0.28	0.29	g
0,200	-3.02	0.77	-1.74	10.48	0	0.13		0.09	0.26	0.28	g
0,200	-3.02	0.77	-1.74	10.48	0	0.13	0.07		0.27	0.28	g
0,300	-3.84	0.82	-1.52	8.04	0	0.14		0.11	0.28	0.30	g
0,300	-3.84	0.82	-1.52	8.04	0	0.14	0.07		0.28	0.29	g
0,400	-4.43	0.88	-1.42	6.95	0	0.12		0.10	0.26	0.28	g
0,400	-4.43	0.88	-1.42	6.95	0	0.12	0.09		0.25	0.26	g
0,500	-4.80	0.92	-1.40	6.73	0	0.12		0.11	0.25	0.27	g
0,500	-4.80	0.92	-1.40	6.73	0	0.12	0.10		0.27	0.28	g
0,750	-5.49	1.02	-1.41	7.95	0	0.16		0.10	0.25	0.27	g
0,750	-5.49	1.02	-1.41	7.95	0	0.16	0.11		0.24	0.26	g
1,000	-5.86	1.09	-1.47	10.26	0	0.16		0.10	0.26	0.28	g
1,000	-5.86	1.09	-1.47	10.26	0	0.16	0.10		0.24	0.26	g
1,490	-6.13	1.15	-1.65	11.97	0	0.21		0.10	0.26	0.28	g
1,490	-6.13	1.15	-1.65	11.97	0	0.21	0.10		0.25	0.27	g
2,000	-6.16	1.15	-1.76	13.69	0	0.23		0.09	0.27	0.28	g
2,000	-6.16	1.15	-1.76	13.69	0	0.23	0.11		0.26	0.28	g

Table 5

PSHV - MI (eq. 3)

T (s)	a	b	c	d	s1	s2	σsta	σeve	σrec	σ tot	unit
0,040	-0.98	0.57	-2.05	10.66	0	0.14		0.11	0.29	0.31	cm/s
0,040	-0.98	0.57	-2.05	10.66	0	0.14	0.10		0.29	0.29	cm/s
0,070	-0.37	0.65	-2.28	14.35	0	0.15		0.09	0.29	0.30	cm/s
0,070	-0.37	0.65	-2.28	14.35	0	0.15	0.11		0.31	0.31	cm/s
0,100	-0.63	0.70	-2.10	12.87	0	0.20		0.10	0.29	0.31	cm/s
0,100	-0.63	0.70	-2.10	12.87	0	0.20	0.09		0.28	0.28	cm/s
0,150	-0.72	0.76	-2.05	13.09	0	0.23		0.11	0.29	0.31	cm/s
0,150	-0.72	0.76	-2.05	13.09	0	0.23	0.11		0.30	0.30	cm/s
0,200	-0.98	0.80	-1.96	12.07	0	0.25		0.10	0.29	0.31	cm/s
0,200	-0.98	0.80	-1.96	12.07	0	0.25	0.11		0.29	0.29	cm/s
0,300	-1.46	0.85	-1.83	10.13	0	0.24		0.10	0.28	0.30	cm/s
0,300	-1.46	0.85	-1.83	10.13	0	0.24	0.09		0.31	0.31	cm/s
0,400	-1.94	0.91	-1.72	9.00	0	0.23		0.10	0.29	0.31	cm/s
0,400	-1.94	0.91	-1.72	9.00	0	0.23	0.09		0.31	0.31	cm/s
0,500	-2.36	0.96	-1.62	8.01	0	0.20		0.08	0.28	0.29	cm/s
0,500	-2.36	0.96	-1.62	8.01	0	0.20	0.09		0.31	0.31	cm/s
0,750	-2.55	1.02	-1.72	9.47	0	0.19		0.12	0.28	0.30	cm/s
0,750	-2.55	1.02	-1.72	9.47	0	0.19	0.11		0.29	0.29	cm/s
1,000	-2.64	1.06	-1.83	10.13	0	0.20		0.10	0.27	0.29	cm/s
1,000	-2.64	1.06	-1.83	10.13	0	0.20	0.08		0.29	0.29	cm/s
1,490	-2.54	1.10	-2.07	11.48	0	0.19		0.11	0.29	0.31	cm/s
1,490	-2.54	1.10	-2.07	11.48	0	0.19	0.10		0.31	0.31	cm/s
2,000	-2.42	1.13	-2.25	12.65	0	0.18		0.11	0.28	0.30	cm/s
2,000	-2.42	1.13	-2.25	12.65	0	0.18	0.10		0.31	0.31	cm/s
3,000	-2.36	1.08	-2.25	11.65	0	0.17		0.10	0.26	0.28	cm/s
3,000	-2.36	1.08	-2.25	11.65	0	0.17	0.09		0.30	0.30	cm/s
4,000	-2.32	1.06	-2.27	11.45	0	0.17		0.11	0.27	0.29	cm/s
4,000	-2.32	1.06	-2.27	11.45	0	0.17	0.09		0.27	0.27	cm/s

Table 6

PSVV - Ml (eq. 3)

T (s)	a	b	c	d	s1	s2	σsta	σeve	σrec	σ tot	unit
0,040	-1.36	0.61	-1.99	9.96	0	0.08		0.10	0.29	0.31	cm/s
0,040	-1.36	0.61	-1.99	9.96	0	0.08	0.10		0.29	0.29	cm/s
0,070	-1.01	0.64	-2.02	10.86	0	0.05		0.10	0.28	0.30	cm/s
0,070	-1.01	0.64	-2.02	10.86	0	0.05	0.10		0.31	0.31	cm/s
0,100	-0.80	0.66	-2.02	12.60	0	0.06		0.11	0.28	0.30	cm/s
0,100	-0.80	0.66	-2.02	12.60	0	0.06	0.09		0.31	0.31	cm/s
0,150	-0.98	0.70	-1.93	12.46	0	0.11		0.09	0.28	0.29	cm/s
0,150	-0.98	0.70	-1.93	12.46	0	0.11	0.08		0.29	0.29	cm/s
0,200	-1.33	0.75	-1.81	10.99	0	0.13		0.10	0.28	0.30	cm/s
0,200	-1.33	0.75	-1.81	10.99	0	0.13	0.08		0.30	0.30	cm/s
0,300	-1.85	0.80	-1.64	9.16	0	0.12		0.10	0.28	0.30	cm/s
0,300	-1.85	0.80	-1.64	9.16	0	0.12	0.08		0.30	0.30	cm/s
0,400	-2.24	0.85	-1.57	8.30	0	0.11		0.11	0.27	0.29	cm/s
0,400	-2.24	0.85	-1.57	8.30	0	0.11	0.08		0.29	0.29	cm/s
0,500	-2.44	0.89	-1.58	7.99	0	0.10		0.11	0.25	0.27	cm/s
0,500	-2.44	0.89	-1.58	7.99	0	0.10	0.08		0.28	0.28	cm/s
0,750	-2.82	0.98	-1.62	9.10	0	0.11		0.10	0.26	0.28	cm/s
0,750	-2.82	0.98	-1.62	9.10	0	0.11	0.08		0.28	0.28	cm/s
1,000	-2.90	1.04	-1.76	11.00	0	0.10		0.10	0.25	0.27	cm/s
1,000	-2.90	1.04	-1.76	11.00	0	0.10	0.08		0.02	0.02	cm/s
1,490	-2.75	1.09	-2.04	12.70	0	0.12		0.10	0.26	0.28	cm/s
1,490	-2.75	1.09	-2.04	12.70	0	0.12	0.08		0.30	0.30	cm/s
2,000	-2.52	1.11	-2.27	14.51	0	0.11		0.11	0.28	0.30	cm/s
2,000	-2.52	1.11	-2.27	14.51	0	0.11	0.09		0.31	0.31	cm/s
3,030	-2.44	1.08	-2.29	11.75	0	0.18		0.09	0.26	0.28	cm/s
3,030	-2.44	1.08	-2.29	11.75	0	0.18	0.10		0.30	0.30	cm/s
4,000	-2.41	1.05	-2.30	12.03	0	0.18		0.10	0.28	0.30	cm/s
4,000	-2.41	1.05	-2.30	12.03	0	0.18	0.11		0.27	0.27	cm/s

Table 7

Mw (eq. 3)

Y (eq.1)	a	b	c	d	s1	s2	σsta	σeve	σrec	σ tot	unit
PGHA	-3.62	0.93	-2.02	11.71	0	0.12		0.10	0.28	0.30	g
PGHA	-3.62	0.93	-2.02	11.71	0	0.12	0.11		0.29	0.31	g
PGVA	-3.49	0.85	-1.99	11.56	0	0.11		0.09	0.29	0.30	g
PGVA	-3.49	0.85	-1.99	11.56	0	0.11	0.12		0.30	0.32	g
PGHV	-3.26	1.07	-1.71	8.32	0	0.18		0.11	0.28	0.30	cm/s
PGHV	-3.26	1.07	-1.71	8.32	0	0.18	0.12		0.29	0.31	cm/s
PGVV	-3.60	1.10	-1.82	9.24	0	0.02		0.10	0.28	0.30	cm/s
PGVV	-3.60	1.10	-1.82	9.24	0	0.02	0.11		0.30	0.32	cm/s
Ia	-5.05	1.88	-3.62	12.98	0	0.46		0.11	0.33	0.35	cm/s
Ia	-5.05	1.88	-3.62	12.98	0	0.46	0.12		0.32	0.34	cm/s
Ih	-2.97	1.20	-2.01	11.80	0	0.22		0.11	0.30	0.32	cm
Ih	-2.97	1.20	-2.01	11.80	0	0.22	0.10		0.31	0.33	cm
DV	-0.94	0.13	0.52	15.60	0	0.03		0.12	0.22	0.25	sec
DV	-0.94	0.13	0.52	15.60	0	0.03	0.11		0.23	0.25	sec

Table 8

SHA - Mw (eq. 3)

T (s)	a	b	c	d	s1	s2	σsta	σeve	σrec	σ tot	unit
0,040	-2.80	0.87	-2.28	12.14	0	-0.13		0.11	0.28	0.30	g
0,040	-2.80	0.87	-2.28	12.14	0	-0.13	0.10		0.31	0.33	g
0,070	-2.50	0.87	-2.31	14.04	0	-0.15		0.09	0.29	0.30	g
0,070	-2.50	0.87	-2.31	14.04	0	-0.15	0.11		0.26	0.28	g
0,100	-2.85	0.90	-2.13	12.83	0	-0.20		0.10	0.30	0.32	g
0,100	-2.85	0.90	-2.13	12.83	0	-0.20	0.09		0.29	0.30	g
0,150	-3.16	0.94	-2.03	12.85	0	-0.23		0.11	0.27	0.29	g
0,150	-3.16	0.94	-2.03	12.85	0	-0.23	0.12		0.28	0.30	g
0,200	-3.65	0.99	-1.91	11.75	0	-0.26		0.11	0.30	0.32	g
0,200	-3.65	0.99	-1.91	11.75	0	-0.26	0.11		0.29	0.31	g
0,300	-4.49	1.05	-1.72	9.03	0	-0.25		0.11	0.30	0.32	g
0,300	-4.49	1.05	-1.72	9.03	0	-0.25	0.12		0.31	0.33	g
0,400	-5.31	1.13	-1.56	7.08	0	-0.25		0.09	0.30	0.31	g
0,400	-5.31	1.13	-1.56	7.08	0	-0.25	0.10		0.29	0.31	g
0,500	-6.00	1.19	-1.42	6.15	0	-0.22		0.10	0.30	0.32	g
0,500	-6.00	1.19	-1.42	6.15	0	-0.22	0.09		0.31	0.32	g
0,750	-6.58	1.24	-1.37	8.59	0	-0.26		0.11	0.29	0.31	g
0,750	-6.58	1.24	-1.37	8.59	0	-0.26	0.09		0.28	0.29	g
1,000	-7.07	1.32	-1.48	8.57	0	-0.23		0.09	0.30	0.31	g
1,000	-7.07	1.32	-1.48	8.57	0	-0.23	0.10		0.28	0.30	g
1,490	-7.50	1.39	-1.60	8.97	0	-0.26		0.10	0.31	0.33	g
1,490	-7.50	1.39	-1.60	8.97	0	-0.26	0.11		0.30	0.32	g
2,000	-7.72	1.41	-1.65	9.91	0	-0.26		0.10	0.29	0.31	g
2,000	-7.72	1.41	-1.65	9.91	0	-0.26	0.09		0.30	0.31	g

Table 9

SVA - Mw (eq. 3)

T (s)	a	b	c	d	s1	s2	σsta	σeve	σrec	σ tot	unit
0,040	-3.00	0.84	-2.16	11.39	0	-0.06		0.10	0.29	0.31	g
0,040	-3.00	0.84	-2.16	11.39	0	-0.06	0.11		0.31	0.33	g
0,070	-2.92	0.82	-2.07	11.18	0	-0.05		0.09	0.30	0.31	g
0,070	-2.92	0.82	-2.07	11.18	0	-0.05	0.09		0.28	0.29	g
0,100	-2.87	0.82	-2.04	12.87	0	-0.07		0.08	0.30	0.31	g
0,100	-2.87	0.82	-2.04	12.87	0	-0.07	0.09		0.29	0.30	g
0,150	-3.36	0.87	-1.91	12.38	0	-0.11		0.12	0.29	0.31	g
0,150	-3.36	0.87	-1.91	12.38	0	-0.11	0.11		0.28	0.30	g
0,200	-4.00	0.93	-1.74	10.33	0	-0.13		0.11	0.31	0.33	g
0,200	-4.00	0.93	-1.74	10.33	0	-0.13	0.10		0.29	0.31	g
0,300	-4.88	0.99	-1.51	7.79	0	-0.13		0.11	0.31	0.33	g
0,300	-4.88	0.99	-1.51	7.79	0	-0.13	0.11		0.31	0.33	g
0,400	-5.54	1.06	-1.40	6.53	0	-0.12		0.09	0.30	0.31	g
0,400	-5.54	1.06	-1.40	6.53	0	-0.12	0.11		0.29	0.31	g
0,500	-5.98	1.11	-1.38	6.16	0	-0.12		0.10	0.28	0.30	g
0,500	-5.98	1.11	-1.38	6.16	0	-0.12	0.12		0.31	0.33	g
0,750	-6.80	1.23	-1.40	7.61	0	-0.15		0.12	0.29	0.31	g
0,750	-6.80	1.23	-1.40	7.61	0	-0.15	0.10		0.28	0.30	g
1,000	-7.25	1.31	-1.46	10.05	0	-0.16		0.09	0.30	0.31	g
1,000	-7.25	1.31	-1.46	10.05	0	-0.16	0.09		0.31	0.32	g
1,490	-7.61	1.39	-1.65	11.84	0	-0.20		0.10	0.29	0.31	g
1,490	-7.61	1.39	-1.65	11.84	0	-0.20	0.08		0.30	0.31	g
2,000	-7.67	1.40	-1.76	13.59	0	-0.23		0.11	0.28	0.30	g
2,000	-7.67	1.40	-1.76	13.59	0	-0.23	0.09		0.31	0.32	g

Table 10

PSHV - Mw (eq. 3)

T (s)	a	b	c	d	s1	s2	σsta	σeve	σrec	σ tot	unit
0,040	-1.74	0.69	-2.04	10.42	0	0.14		0.11	0.30	0.32	cm/s
0,040	-1.74	0.69	-2.04	10.42	0	0.14	0.12		0.29	0.31	cm/s
0,070	-1.21	0.79	-2.27	14.21	0	0.15		0.10	0.32	0.34	cm/s
0,070	-1.21	0.79	-2.27	14.21	0	0.15	0.11		0.29	0.31	cm/s
0,100	-1.52	0.85	-2.10	12.75	0	0.20		0.11	0.28	0.30	cm/s
0,100	-1.52	0.85	-2.10	12.75	0	0.20	0.10		0.29	0.31	cm/s
0,150	-1.69	0.91	-2.04	12.95	0	0.23		0.12	0.29	0.31	cm/s
0,150	-1.69	0.91	-2.04	12.95	0	0.23	0.11		0.28	0.30	cm/s
0,200	-2.01	0.97	-1.95	11.91	0	0.25		0.12	0.29	0.31	cm/s
0,200	-2.01	0.97	-1.95	11.91	0	0.25	0.12		0.30	0.32	cm/s
0,300	-2.55	1.03	-1.83	10.01	0	0.23		0.11	0.31	0.33	cm/s
0,300	-2.55	1.03	-1.83	10.01	0	0.23	0.09		0.29	0.30	cm/s
0,400	-3.11	1.10	-1.71	8.75	0	0.22		0.10	0.28	0.30	cm/s
0,400	-3.11	1.10	-1.71	8.75	0	0.22	0.11		0.28	0.30	cm/s
0,500	-3.57	1.16	-1.62	8.00	0	0.20		0.11	0.29	0.31	cm/s
0,500	-3.57	1.16	-1.62	8.00	0	0.20	0.12		0.30	0.32	cm/s
0,750	-3.86	1.24	-1.73	9.45	0	0.18		0.12	0.28	0.30	cm/s
0,750	-3.86	1.24	-1.73	9.45	0	0.18	0.10		0.27	0.29	cm/s
1,000	-4.02	1.29	-1.83	10.07	0	0.19		0.11	0.29	0.31	cm/s
1,000	-4.02	1.29	-1.83	10.07	0	0.19	0.08		0.31	0.32	cm/s
1,490	-3.97	1.34	-2.07	11.49	0	0.18		0.09	0.28	0.29	cm/s
1,490	-3.97	1.34	-2.07	11.49	0	0.18	0.10		0.30	0.32	cm/s
2,000	-3.89	1.38	-2.26	12.69	0	0.18		0.10	0.29	0.31	cm/s
2,000	-3.89	1.38	-2.26	12.69	0	0.18	0.12		0.29	0.31	cm/s
3,000	-3.13	1.23	-2.28	12.23	0	0.18		0.09	0.30	0.31	cm/s
3,000	-3.13	1.23	-2.28	12.23	0	0.19	0.11		0.30	0.32	cm/s
4,000	-3.05	1.17	-2.32	11.98	0	0.19		0.12	0.29	0.31	cm/s
4,000	-3.05	1.17	-2.32	11.98	0	0.19	0.10		0.28	0.30	cm/s

Table 11

PSVV - Mw (eq. 3)

T (s)	a	b	c	d	s1	s2	σsta	σeve	σrec	σ tot	unit
0,040	-2.17	0.74	-1.97	9.57	0	0.08		0.12	0,28	0,30	cm/s
0,040	-2.17	0.74	-1.97	9.57	0	0.08	0.11		0,28	0,30	cm/s
0,070	-1.84	0.78	-2.00	10.54	0	0.07		0.10	0,29	0,31	cm/s
0,070	-1.84	0.78	-2.00	10.54	0	0.07	0.12		0,30	0,32	cm/s
0,100	-1.63	0.79	-2.01	12.41	0	0.07		0.09	0,29	0,30	cm/s
0,100	-1.63	0.79	-2.01	12.41	0	0.07	0.11		0,28	0,30	cm/s
0,150	-1.87	0.85	-1.92	12.31	0	0.11		0.11	0,29	0,31	cm/s
0,150	-1.87	0.85	-1.92	12.31	0	0.11	0.11		0,30	0,32	cm/s
0,200	-2.29	0.90	-1.80	10.83	0	0.12		0.12	0,30	0,32	cm/s
0,200	-2.29	0.90	-1.80	10.83	0	0.12	0.09		0,29	0,30	cm/s
0,300	-2.86	0.96	-1.63	9.00	0	0.12		0.10	0,30	0,32	cm/s
0,300	-2.86	0.96	-1.63	9.00	0	0.12	0.12		0,30	0,32	cm/s
0,400	-3.32	1.03	-1.56	8.01	0	0.11		0.12	0,29	0,31	cm/s
0,400	-3.32	1.03	-1.56	8.01	0	0.11	0.09		0,30	0,31	cm/s
0,500	-3.59	1.07	-1.57	7.56	0	0.09		0.10	0,31	0,33	cm/s
0,500	-3.59	1.07	-1.57	7.56	0	0.09	0.12		0,28	0,30	cm/s
0,750	-4.08	1.18	-1.61	8.90	0	0.11		0.11	0,30	0,32	cm/s
0,750	-4.08	1.18	-1.61	8.90	0	0.11	0.11		0,30	0,32	cm/s
1,000	-4.24	1.26	-1.76	10.90	0	0.10		0.10	0,31	0,33	cm/s
1,000	-4.24	1.26	-1.76	10.90	0	0.10	0.09		0,29	0,30	cm/s
1,490	-4.17	1.33	-2.04	12.69	0	0.11		0.12	0,29	0,31	cm/s
1,490	-4.17	1.33	-2.04	12.69	0	0.11	0.11		0,30	0,32	cm/s
2,000	-3.98	1.36	-2.28	14.57	0	0.11		0.10	0,28	0,30	cm/s
2,000	-3.98	1.36	-2.28	14.57	0	0.11	0.11		0,30	0,32	cm/s
3,030	-3.77	1.28	-2.28	12.14	0	0.12		0.11	0,29	0,31	cm/s
3,030	-3.77	1.28	-2.28	12.14	0	0.12	0.12		0,30	0,32	cm/s
4,000	-3.42	1.22	-2.33	12.36	0	0.10		0.10	0,29	0,31	cm/s
4,000	-3.42	1.22	-2.33	12.36	0	0.10	0.10		0,28	0,30	cm/s

Table 12